Wang and Guo
Carbon Balance and Management (2025) 20:7
https://doi.org/10.1186/s13021-025-00301-8

Carbon Balance and Management

RESEARCH

Open Access

Forecasting CO_2 emissions in BRICS countries using the grey breakpoint prediction models

Huiping Wang[1*] and Xinge Guo[1]

Abstract

In this paper, three novel grey breakpoint prediction models are proposed based on calculating the development coefficient and grey action of grey prediction models after fuzzy breakpoints, unifying the calculation methods for parameter estimation and the relevant time-response equations, and using the particle swarm optimisation algorithm to optimise the two-stage background values. Finally, the novel grey breakpoint prediction models are used to simulate and forecast the CO_2 emissions in BRICS countries. We can see that by setting time breakpoints and fuzzy breakpoint intervals, the novel methods successfully detect abrupt changes in the system and achieve accurate predictions, thus improving the accuracy and applicability of the grey model. The new grey breakpoint prediction models demonstrate better estimation in all cases in CO_2 emissions forecasting. The projections show that between 2022 and 2025, CO_2 emissions in Brazil and South Africa will decrease each year, while CO_2 emissions in China, Russia and India will increase each year, but the upwards trend in India shows signs of slowing.

Keywords Grey breakpoint prediction model, Particle swarm optimisation, CO_2 emissions, Time response function

Introduction

Global climate change has emerged as one of the most formidable challenges in the twenty-first century, with CO_2 emissions, as the primary source of greenhouse gases, directly impacting the sustainable development and climate governance effectiveness of all nations. As representatives of emerging economies, BRICS countries have witnessed a continuous increase in energy consumption and CO_2 emissions amidst rapid industrialization and urbanization processes [1]. According to data from the IEA, BRICS countries account for over 40% of the global total CO_2 emissions, and their emission reduction pathways are decisive for achieving the temperature control goals set out in the Paris Agreement. With the sustained and rapid economic growth and accelerated urbanization of BRICS countries, energy demand continues to rise, and industrial structures are continuously upgraded, leading to an upward trend in CO_2 emissions. However, significant disparities exist among BRICS countries in terms of economic development levels, energy structures, industrial structures, and emission reduction technologies. This heterogeneity renders the driving factors and variation patterns of their CO_2 emissions complex and diverse, thereby increasing the difficulty of accurate prediction [2].

Currently, there are a variety of methods that have been applied to obtain carbon emission projections, mainly including the following types. First, macroeconomic system models treat an energy system as a sector of the macroeconomic system, and as economic growth impacts this sector, macroeconomic changes will lead to changes in the supply and demand of the energy system, so as to measure the interaction between the energy system and other systems and the impacts of emission reduction policies on the national macro-economy, mainly including the input–output models and (computable general equilibrium) CGE models [3–5]. Second, statistical

*Correspondence:
Huiping Wang
wanghuiping@xaufe.edu.cn
[1] Western Collaborative Innovation Research Center for Energy Economy and Regional Development, Xi'an University of Finance and Economics, Xi'an 710100, China

analysis models, which consider the effects of economic development, resource endowments, low-carbon technology, environmental regulations and other factors on CO_2 emissions and decompose these factors before making predictions, such as the impact-population-affluence-technology (IPAT) [6], stochastic impacts by regression on population, affluence, and technology (STIRPAT) [7], long-range energy alternatives planning system (LEAP) [8], multiple regression analysis synthesis methods [9], and other models are used. Third, artificial intelligence models, which can identify the intrinsic characteristics in historical carbon emission datasets, can be modified in real time to improve the accuracy of predictions. These models include artificial neural network (ANN) [10], generalised regression neural network (GRNN) [11], back propagation neural network (BPNN) [7], support vector machines (SVMs) [12], extreme learning machines [13], Elman neural network [14], long short-term memory networks (LSTMNs) [15]. The fourth type are grey prediction models. Most of the forecasting methods mentioned above require a large amount of sample data or must consider the factors that influence CO_2 emissions; thus, the amount of data available and the number of variables considered will affect the accuracy of forecasting. However, for variables such as CO_2 emissions, for which only short-term data are valid and the influencing factors are complex, the above methods often require long timescales for data collection, and certain data might prove challenging or even unattainable to gather. The grey model is a good solution to these problems, as it can be used to build prediction models for systems with limited data without considering the influence of other factors; therefore, this method has considerable advantages in cases with insufficient validation data, and it has been widely used for carbon emission prediction in different fields [16, 17]. Additionally, due to their straightforward structure, extensive applicability, minimal sample size requirements, and high precision, grey forecasting models are widely used in cases involving GDP and population [18], energy imports demand [19], quarterly crude oil production and coke production [20], clean energy [21], green transformation of manufacturing industry [22], crude oil production [23], electricity transformer's seasonal oil temperature [24], transport performance of civil aviation industry [25], oil reserves [26], innovation performance in high-tech industries[27], electricity consumption [28], construction waste [29], rainstorm days [30], health of lithium battery [31], etc.

Early grey models were often limited by the inadequate use of new information, and they neglected time lags in data and system shocks. Scholars have continuously optimised and improved these models, and the main improvements are as follows. First, background value optimisation was performed. Because the traditional background values are constructed using data adjacent to the mean, the magnitude of the background value is easily affected by certain extreme values in the original series, and this approach is mainly applicable to small-sample time series with gradual changes, making it fairly limited; therefore, scholars have optimised the background value construction method from different perspectives. For example, background value optimisation has been combined with initial term optimisation [32], genetic algorithms have been used to optimise the weighting coefficients of background values with a nonlinear time correction factor [33], generic optimisation-based forms of background values have been applied [34], and background values have been optimised in stages based on minimising weighting errors [35]. Second, the cumulative approach has been improved. To increase the weight of new information, a fractional-order grey model was introduced, and it can reflect the priority of new information and generalize cumulative integer generation, with much better predictive performance than the integer-order grey model [36]. Since then, a large number of fractional-order grey prediction models have been proposed based on fractional-order cumulants, such as the fractional-order adaptive intelligent grey model [37], fractional-order nonlinear Bernoulli model [38], grey model with conformable fractional opposite-direction accumulation [39], fractional-order grey kernel model [40], conformable fractional-order grey model [41], and generalised fractional grey model [42]. To effectively use new information, reverse cumulative generation techniques have been introduced into grey models [43], conformable fractional reverse grey models [44], and adaptive reverse cumulative discrete grey models with time power terms [45]. Additionally, the damped cumulative generating operator, the weakened fractional-order cumulative operator, and the Grunwald–Letnikov fractional-order sequence generating operator were proposed to flexibly adjust the predictions of grey models [46–48]. Third, the original model structure has been extended. To improve the fitting performance of grey models for different types of data, scholars have extended the structure of the GM(1,1). For example, the GM(1, N|sin) was proposed to address the nonlinear relationship between and periodic oscillations of independent and dependent variables [49]. Furthermore, nonlinear and periodic components were integrated into the framework to accurately capture the evolving trends within time series data, thereby enhancing the grey model's adaptability to handle arbitrary periodic patterns [50]. For seasonal data, a pioneering seasonal model was developed by embedding categorical dummy variables within the model architecture, enabling precise identification and

modelling of seasonal fluctuations [51]. A novel structural adaptive grey model combined with a data stacking technique was proposed to solve time series forecasting problems characterised by seasonality, nonlinearity and uncertainty [52]. In addition, several excellent grey models have been created based on extended model structures, such as the fractional time-delayed grey Bernoulli forecasting model (FBTDGM) [53], the fractional grey Gompertz model [54], the grey seasonal model based on cycle accumulation generation (CDGSM) [55], and the discrete grey seasonal model with the time power term (DGSTPM) [20]. Fourth, methods for prioritizing new information have been proposed. In the GM(1,1), equal weights are assigned to new information and old information; obviously, this is not reasonable. Therefore, to improve the prediction accuracy, the new information can be flexibly given higher weights [56]. For example, an exponential parameter was introduced, an optimisation algorithm was used to find the optimal parameter value, and the weight of the information was set by adjusting the size of the parameter [1]. Since new information has a large impact on the trend of the results, a new information-weighted cumulative generation operator was adopted [57]. A flexible dynamic fractional-order accumulation operator that utilises a dynamic nonlinear incomplete gamma function was developed to effectively exploit the more recent information hidden in a given time series [58]. A new cumulative operator incorporating a dynamic weight adjustment factor was proposed to enhance the timeliness of new information utilisation in grey forecasting methods [50]. Additionally, a rolling mechanism was introduced in the modelling procedure to prioritise the use of new information [59, 60]. Fifth, combinatorial models have been constructed. With the development of grey models, to avoid inconsistent accuracy due to improper model selection, combining forecasting models has become a good choice. Notably, grey models have been combined with other forecasting models to improve the accuracy and stability of forecasting, such as by combining autoregressive integrated moving average (ARIMA) and metabolic nonlinear grey model (MNGM) [61], combining volatile grey forecasting models and ARMA/RW models [62], combining GM(1,1) and linear weighted average mixed model [63], combining fuzzy information granulation (FIG) and grey autoregressive model (GARM) [64], and combining grey model and convolutional neural network [65]. In general, the combined models can be modified in real time based on the intrinsic mathematical characteristics of historical data series, thus effectively avoiding the shortcomings arising from the use of a single model to describe the trends of complex time series and greatly improving the prediction accuracy [66].

The above research has not only broadened the application of grey prediction models but also improved the prediction accuracy in many cases; however, the existing models tend to ignore changes in system operation and disturbances to external contingencies. Therefore, Zhang and Wang [67] added the time breakpoints to the GM(1,1) and constructed two novel grey breakpoint models GBPM(1,1,t) and OGBPM(1,1,t). These models consider fluctuations in the system as a whole and changes in the system development trend. However, the setting of breakpoints is relatively subjective, which can significantly limit the application of the model, and the parameter estimation method used can lead to large model errors. The effects of disturbances tend to last for some time, and the impact of these external shocks on the future trend of a system may display a time lag. Therefore, in this paper, to avoid misjudging the time breakpoints and enhance the forecasting accuracy and applicability of the traditional model, three new grey breakpoint prediction models are established by introducing the grey prediction model development coefficient a and grey action b after the fuzzy breakpoints. These models are the NOGBPM(1,1,t), NGBPM(1,1,t) and AGBPM(1,1,t). By comparing the new models with GM(1,1), FGM(1,1,r), GBPM(1,1,t) and OGBPM(1,1,t) in the simulation and prediction of CO_2 emissions in BRICS countries, the new models are tested and validated. Several contributions can be made as follows:

(1) It is assumed that the breakpoint $t*$ is not a fixed time but a time interval, and the optimal breakpoint t_m within this interval is then determined according to the model fitting result and prediction accuracy. Subsequently, three new grey breakpoint prediction models are established: NOGBPM, NGBPM, and AGBPM.
(2) The parameter estimation method is optimised, and parameters are determined without differentiating data before or after a breakpoint; thus, all the original data can be fully utilised when determining the parameters. This approach improves the accuracy of the parameters and the prediction results.
(3) Since the data trends before the optimal breakpoint t_m and after t_m will change greatly, a two-stage background value calculation method is introduced into the model, and the optimal background values before and after the breakpoint are determined with the PSO algorithm.
(4) The validity and applicability of the three new models are verified using historical CO_2 emission data from BRICS countries, and the CO_2 emissions of the BRICS countries are projected for the period of 2022–2025.

This study is organised as follows. In Sect. Construction of grey breakpoint models, the establishment, optimisation and properties of the novel grey breakpoint models are discussed, and error measures and validity tests are introduced. In Sect. Validation of the grey breakpoint prediction models, utilizing the CO_2 emission data of the BRICS countries, the GM, FGM, GBPM and OGBPM models, along with three newly constructed models, are employed for modelling. The prediction accuracy of these seven grey models is compared, thereby validating the effectiveness and adaptability of the novel grey breakpoint models. Section Application in forecasting the CO_2 emissions of BRICS countries presents the projections of CO_2 emissions in BRICS countries for the period of 2022–2025 and Sect. Conclusion offers the conclusions and policy implications drawn from the findings.

Construction of grey breakpoint models

Basic concept

Suppose the original sequence is $X^{(0)} = \left(x^{(0)}(1),\ x^{(0)}(2),\ \cdots,\ x^{(0)}(n)\right)^T$ and the sequence $X^{(1)} = \left(x^{(1)}(1),\ x^{(1)}(2),\ \cdots,\ x^{(1)}(n)\right)^T$ is obtained by the first-order cumulative generation operator 1-AGO, where

$$x^{(1)}(k) = \sum_{i=1}^{k} x^{(0)}(i), k = 1, 2..., n \tag{1}$$

The sequence $Z^{(1)} = \left(z^{(1)}(2),\ z^{(1)}(3),\ \cdots,\ z^{(1)}(n)\right)^T$ is the mean sequence of $X^{(1)}$, where

$$z^{(1)}(k) = \frac{x^{(1)}(k) + x^{(1)}(k-1)}{2}, k = 2, 3, \cdots n \tag{2}$$

Definition 1: The basic form of the grey forecasting model GM(1,1) is

$$x^{(0)}(k) + az^{(1)}(k) = b \tag{3}$$

Definition 2: Assuming that external shocks affect the future dynamics of a system at time t^*, the basic form of the grey breakpoint prediction model GBPM(1,1,t) is

$$x^{(0)}(k) + az^{(1)}(k) = b + c \times \phi \tag{4}$$

$$\phi = \begin{cases} 1, k \geq t^* \\ 0, k < t^* \end{cases}$$

where a is the development coefficient, b is the grey action, ϕ is a dummy variable assigned a value of 0 or 1, which is set based on whether a shock occurs or not. c is the coefficient of mutation, which represents the correction to the grey action of the original model after the occurrence of a shock and reflects the impact of external shocks on the system. The process of solving parameters is as follows.

When $k < t^*$, $\left[\begin{array}{cc} a & b \end{array}\right]^T$ are estimated using the least square method (LSM), as follows.

$$\left[\begin{array}{c} \hat{a} \\ \hat{b} \end{array}\right] = (B^T B)^{-1} B^T Y \tag{5}$$

$$B = \left[\begin{array}{cc} -z^{(1)}(2) & 1 \\ -z^{(1)}(3) & 1 \\ \vdots & \vdots \\ -z^{(1)}(t^*-1) & 1 \end{array}\right], \quad Y = \left[\begin{array}{c} x^{(0)}(2) \\ x^{(0)}(3) \\ \vdots \\ x^{(0)}(t^*-1) \end{array}\right] \tag{6}$$

When $k \geq t^*$, the LSM is used directly to estimate the parameter c, i.e.,

$$\hat{c} = \min \sum_{k=t^*}^{n} \left(x^{(0)}(k) + \hat{a}z^{(1)}(k) - \hat{b} - c\right)^2 \tag{7}$$

Then, according to a whitening equation,

$$\frac{dx^{(1)}}{dt} + ax^{(1)} = b + c \times \phi \tag{8}$$

Now, the time response equation is obtained:

$$\begin{aligned} \hat{x}^{(1)}(k) = (x^{(1)}(t^*-1) - \frac{b + c \times \phi}{a})e^{-a(k-t^*+1)} \\ + \frac{b + c \times \phi}{a}, k = 1, 2, \cdots n \end{aligned} \tag{9}$$

Definition 3: The basic form of the optimised grey breakpoint prediction model OGBPM(1,1,t) is

$$x^{(0)}(k) + (a + \varepsilon \times \phi)z^{(1)}(k) = b + c \times \phi \tag{10}$$

$$\phi = \begin{cases} 1, k \geq t^* \\ 0, k < t^* \end{cases}$$

where a, b, c and ϕ have the same meanings as above. ε is the coefficient of change in development, which represents the correction to the original model development coefficient after a shock has occurred and reflects the shocks' influence on the system's development trend. The model is established in the same way as above, except for the estimation of parameters ε and c. The parameters are determined as follows.

When $k \geq t^*$, the simulated ensemble value is expressed as

$$x^{(0)}(k+1) = e^{-(\hat{\alpha}+\hat{\varepsilon})}x^{(0)}(k), k \geq t^* \tag{11}$$

According to Eq. (12), the parameter ε can be calculated as

$$\varepsilon = \min \sum_{k=t^*}^{n-1} (x^{(0)}(k+1) - e^{-(\hat{\alpha}+\varepsilon)}x^{(0)}(k))^2$$

$$\varepsilon = -\ln\left((B^T B)^{-1}B^T Y\right) - \hat{a} \tag{12}$$

$$B = \begin{bmatrix} x^{(0)}(t^*) \\ x^{(0)}(t^*+1) \\ \vdots \\ x^{(0)}(n-1) \end{bmatrix}, \quad Y = \begin{bmatrix} x^{(0)}(t^*+1) \\ x^{(0)}(t^*+2) \\ \vdots \\ x^{(0)}(n) \end{bmatrix}$$

Thus, based on ε, the optimal estimate of c is

$$\hat{c} = (\hat{a}+\varepsilon)(x^{(1)}(t^*-1) - \frac{\sum_{k=t^*}^{n} x^{(0)}(k)e^{-(\hat{a}+\varepsilon)(k-t^*+1)}}{\left(1-e^{(\hat{a}+\varepsilon)}\right)\sum_{k=t^*}^{n} e^{-2(\hat{a}+\varepsilon)(k-t^*+1)}}) - \hat{b} \tag{13}$$

However, the above process of solving for the parameters comes with jump errors, and c and ε do not fully utilise all information associated with the original data, leading to significant biases. Additionally, when the length of time after a breakpoint is extremely short, i.e., when the available data are insufficient, it is difficult to guarantee the accuracy of the parameters and predictions by the LSM. Therefore, a unified calculation method is proposed for parameter estimation, making the parameter solutions easier to obtain and enhances the novel grey breakpoint model.

Novel grey breakpoint prediction models

Based on the above construction of GBPM(1,1,t) and OGBPM(1,1,t), the fuzzy breakpoint assumptions, parameter estimation methods and background values of the original models are optimised to better simulate shocks and enhance the modelling accuracy, resulting in three novel grey breakpoint prediction models.

The impact of disturbance on the system's future tend may display a time lag. To avoid misjudging the breakpoint of a shock, it is assumed that the breakpoint $t*$ is not a fixed time but a time interval, and the most suitable breakpoint t_m within that interval is determined; therefore, it is assumed that a shock affecting the future dynamics of the system, such as a policy change or economic crisis, occurs at a certain time $t = (t_1, t_2, \cdots, t_s)$, where t_m is the best-fit breakpoint. ϕ is set based on whether a shock occurs or not.

$$\phi = \begin{cases} 1, & k \geq t_m \\ 0, & k < t_m \end{cases} \tag{14}$$

Definition 4: By the OGBPM(1,1,t) model, the corresponding parameter estimation method and fuzzy breakpoint assumptions are improved and the grey action parameter and development trend are adjusted to construct a new optimised grey breakpoint prediction model NOGBPM(1,1,t) in the following basic form.

$$x^{(0)}(k) + (a + \varepsilon \times \phi)z^{(1)}(k) = b + c \times \phi \tag{15}$$

Definition 5: Based on the GBPM(1,1,t) model, the appropriate parameter estimation method and fuzzy breakpoint assumptions are improved and the grey action parameter is adjusted to construct a new grey breakpoint prediction model NGBPM(1,1,t), which has the following basic form.

$$x^{(0)}(k) + az^{(1)}(k) = b + c \times \phi \tag{16}$$

Definition 6: The basic form of AGBPM(1,1,t) model with fuzzy breakpoint assumptions and modified development trends is as follows.

$$x^{(0)}(k) + (a + \varepsilon \times \phi)z^{(1)}(k) = b \tag{17}$$

NOGBPM(1,1,t) is used as an example to further explain the parameter solutions, time response equation, final reduced equation and optimal time breakpoint. NGBPM(1,1,t) and AGBPM(1,1,t) are based on the same process.

The basic form of NOGBPM(1,1,t) can also be written in the form of a segmented function:

$$\begin{cases} x^{(0)}(2) + (a+0)z_1^{(1)}(2) = 1 \cdot b + 0 \cdot c \\ \vdots \\ x^{(0)}(t_m - 1) + (a+0)z_1^{(1)}(t_m - 1) = 1 \cdot b + 0 \cdot c \\ x^{(0)}(t_m) + (a+\varepsilon)z_2^{(1)}(t_m) = 1 \cdot b + 1 \cdot c \\ \vdots \\ x^{(0)}(n) + (a+\varepsilon)z_2^{(1)}(n) = 1 \cdot b + 1 \cdot c \end{cases} \tag{18}$$

The estimation of parameters with the LSM is as follows.

$$\hat{p} = (\hat{a}, \hat{\varepsilon}, \hat{b}, \hat{c})^T = (B^T B)^{-1}B^T Y \tag{19}$$

$$B=\begin{pmatrix} -z_1^{(1)}(2) & 0 & 1 & 0 \\ \vdots & \vdots & \vdots & \vdots \\ -z_1^{(1)}(t_m-1) & 0 & 1 & 0 \\ -z_2^{(1)}(t_m) & -z_2^{(1)}(t_m) & 1 & 1 \\ \vdots & \vdots & \vdots & \vdots \\ -z_2^{(1)}(n) & -z_2^{(1)}(n) & 1 & 1 \end{pmatrix} \quad Y=\begin{bmatrix} x^{(0)}(2) \\ x^{(0)}(3) \\ \vdots \\ x^{(0)}(n) \end{bmatrix}$$

The whitening equation for this model is

$$\frac{dx^{(1)}}{dt}+(a+\varepsilon\times\phi)x^{(1)}=b+c\times\phi \tag{20}$$

Alternatively, this equation can be expressed as

$$\begin{cases} \dfrac{dx^{(1)}(k)}{dt}+ax^{(1)}(k)=b \quad k<t_m \\ \dfrac{dx^{(1)}(k)}{dt}+(a+\varepsilon)x^{(1)}(k)=b+c \quad k\geq t_m \end{cases}$$

Based on the whitening equation, the time response equation is established

$$\hat{x}^{(1)}(k)=Ce^{-(a+\varepsilon\times\phi)(k-1)}+\frac{b+c\times\phi}{a+\varepsilon\times\phi},k=1,2,\cdots n \tag{21}$$

where C is the unknown constant, and according to the priority of new information and to effectively reflect the segmented nature of the NOGBPM(1,1,t), the cumulative data before the best-fit breakpoint are used as the initial values to obtain the time response:

$$\hat{x}^{(1)}(k)=(x^{(1)}(t_m-1)-\frac{b+c\times\phi}{a+\varepsilon\times\phi})e^{-(a+\varepsilon\times\phi)(k-t_m+1)} +\frac{b+c\times\phi}{a+\varepsilon\times\phi},k=1,2, \quad n \tag{22}$$

Finally, the reduced modelling equation can be obtained according to the cumulative reduction formula.

$$\hat{x}^{(0)}(k)=\hat{x}^{(1)}(k)-\hat{x}^{(1)}(k-1),k=2,3,\cdots,n \tag{23}$$

$$\begin{cases} \hat{x}^{(0)}(k)=\left(1-e^{\hat{a}}\right)\left(x^{(1)}(t_m-1)-\dfrac{\hat{b}}{\hat{a}}\right)e^{-\hat{a}(k-t_m+1)} \quad k<t_m \\ \hat{x}^{(0)}(k)=\left(1-e^{(\hat{a}+\hat{\varepsilon})}\right)\left(x^{(1)}(t_m-1)-\dfrac{\hat{b}+\hat{c}}{\hat{a}+\hat{\varepsilon}}\right)e^{-(\hat{a}+\hat{\varepsilon})(k-t_m+1)} \quad k\geq t_m \end{cases}$$

An optimal breakpoint t_m is selected by minimising the mean absolute percentage error (MAPE) of the modelled data, and the following are the specific functions.

$$\min MAPE=\frac{1}{n}\sum_{k=1}^{n}\left|\frac{x^{(0)}(k)-\hat{x}^{(0)}(k)}{x^{(0)}(k)}\right|\times 100\% \tag{24}$$

$$s.t.\begin{pmatrix} \hat{p}=(\hat{a},\hat{\varepsilon},\hat{b},\hat{c})^T=(B^TB)^{-1}B^TY \\ \hat{x}^{(1)}(k)=(x^{(1)}(t_m-1)-\frac{b+c\times\phi}{a+\varepsilon\times\phi})e^{-(a+\varepsilon\times\phi)(k-t_m+1)}+\frac{b+c\times\phi}{a+\varepsilon\times\phi} \\ \hat{x}^{(0)}(k)=\hat{x}^{(1)}(k)-\hat{x}^{(1)}(k-1) \\ k=2,3,\cdots,n \end{pmatrix} \tag{25}$$

Optimisation of background values

In the original modelling process, the true value $x^{(1)}(k)$ after differentiation is estimated from the background value $z^{(1)}(k)$, which is calculated based on an approximation,

$$z^{(1)}(k)=\int_{k-1}^{k}x^{(1)}(k)dt\approx\frac{x^{(1)}(k)+x^{(1)}(k-1)}{2},k=2,3,\cdots n \tag{26}$$

which is one of the main reasons for the error. Moreover, because the original data studied in this paper are segmented, the two-stage background value calculation methods used, and the optimisation of the background value is also segmented to best consider the breakpoint characteristics of the model and prioritise new information in the modelling process. Next, we set $\alpha,\beta\in\left[0,\ 1\right]$, as follows.

$$\begin{aligned} z_1^{(1)}(k)&=\int_{k-1}^{k}x^{(1)}(t)dt=\alpha x(k-1)+(1-\alpha)x(k),k<t_m \\ z_2^{(1)}(k)&=\int_{k-1}^{k}x^{(1)}(t)dt=\beta x(k-1)+(1-\beta)x(k),k\geq t_m \end{aligned} \tag{27}$$

The optimal values of the parameters α and β can be obtained using an optimisation algorithm. In this paper, PSO is chosen to calculate the above two unknown parameters to minimise the MAPE of the model-fitted data. Based on NOGBPM(1,1,t), only one of the parameters c or ε needs to be removed to obtain NGBPM(1,1,t) or AGBPM(1,1,t).

$$\min MAPE=\frac{1}{n}\sum_{k=1}^{n}\left|\frac{x^{(0)}(k)-\hat{x}^{(0)}(k)}{x^{(0)}(k)}\right|\times 100\% \tag{28}$$

$$s.t.\begin{pmatrix} z_1^{(1)}(k)=\alpha x(k-1)+(1-\alpha)x(k),k<t_m \\ z_2^{(1)}(k)=\beta x(k-1)+(1-\beta)x(k),k\geq t_m \\ \hat{p}=(\hat{a},\hat{\varepsilon},\hat{b},\hat{c})^T=(B^TB)^{-1}B^TY \\ \hat{x}^{(1)}(k)=(x^{(1)}(t_m-1)-\frac{b+c\times\phi}{a+\varepsilon\times\phi})e^{-(a+\varepsilon\times\phi)(k-t_m+1)}+\frac{b+c\times\phi}{a+\varepsilon\times\phi} \\ \hat{x}^{(0)}(k)=\hat{x}^{(1)}(k)-\hat{x}^{(1)}(k-1) \\ k=2,3,\cdots,n \end{pmatrix} \tag{29}$$

Adaptabilities of the novel models

Although the aforementioned three models exhibit relative consistency in terms of formulas and calculations, they differ in nature and are applicable to distinct scenarios, which are described below.

Scenario 1: When the coefficients $\varepsilon = 0$, $c = 0$, $\alpha = 0.5$, and $\beta = 0.5$, the above three models are consistent with GM(1,1) and provide good compatibility.

The meanings of a and b are consistent with traditional grey models. c is the coefficient of mutation, which represents the modification of the grey action of the original model after the occurrence of a shock. ε is the coefficient of change in development, which represents the modification of the development coefficient of the original model after the occurrence of a shock and reflects the shock's influence on the system. When there are no external shocks to the system, the above three models evolve into the traditional grey model.

Scenario 2: The three grey breakpoint prediction models are effectively used to evaluate the effects of external disturbances from different perspectives.

In the process of building the NOGBPM(1,1,t), both the development coefficient and the grey action are modified based on the segmented data, which can lead to the overly fragmented treatment of information before and after a breakpoint. Notably, in overfragmentation, the prediction of future information is based only on the information after the breakpoint. If the information after the breakpoint is limited, it is difficult to guarantee the prediction accuracy. Therefore, the AGBPM(1,1,t) model corrected only for the a and NGBPM(1,1,t) corrected only for the b are proposed to account for the effects of external disturbances.

Scenario 3: The effects of external shock on the system are characterised by phases, diversity and time lags, and the three grey breakpoint forecasting models can reflect these characteristics with good accuracy.

To reflect the influence of stage, the background values are optimised paper by differentiating stages before and after breakpoints and determining the relevant parameters with PSO to obtain different background values. To address the effect of diversity, the influence of shocks on the a and b is considered. To best fit the original data, these three grey breakpoint prediction models are compared, and the model with the lowest fitting error is selected to predict the future development trend of the system. To avoid the errors caused by time lags, a breakpoint is set as a period with a fuzzy interval, and the optimal breakpoint is determined by calculating the minimum comprehensive error. This approach improves the prediction accuracy.

Error metrics

As the raw data in this paper are divided into pre-breakpoint and post-breakpoint components in the modelling process, the segmented data must also be assessed to calculate the pre-breakpoint fit, post-breakpoint fit, prediction accuracy and combined error based on different error metrics. In the simulation phase, the mean absolute percentage error before a breakpoint (BMAPE), mean absolute percentage error after a breakpoint (AMAPE) and mean absolute percentage error of simulation (MAPE) are used to calculate the simulation error of the model, as follows:

$$BMAPE = \frac{1}{t-1}\sum_{k=1}^{t-1}\left|\frac{x^{(0)}(k)-\hat{x}^{(0)}(k)}{x^{(0)}(k)}\right| \times 100\% \tag{30}$$

$$AMAPE = \frac{1}{n-t+1}\sum_{k=t}^{n}\left|\frac{x^{(0)}(k)-\hat{x}^{(0)}(k)}{x^{(0)}(k)}\right| \times 100\% \tag{31}$$

$$MAPE = \frac{1}{n}\sum_{k=1}^{n}\left|\frac{x^{(0)}(k)-\hat{x}^{(0)}(k)}{x^{(0)}(k)}\right| \times 100\% \tag{32}$$

where t is the time breakpoint. The background value is optimised with the condition that MAPE is minimised; i.e., when the PSO algorithm is used to calculate the background value, the output parameter is that which minimizes the MAPE. The mean absolute percentage error of prediction (FMAPE) is applied to analyse the prediction error, which is given by

$$FMAPE = \frac{1}{f}\sum_{k=n+1}^{n+f}\left|\frac{x^{(0)}(k)-\hat{x}^{(0)}(k)}{x^{(0)}(k)}\right| \times 100\% \tag{33}$$

where f is the number of prediction periods. As the aim of improving the model is to achieve increased forecasting accuracy, the FMAPE is also an important indicator for determining the effectiveness of the model. To indicate the overall fit of the model in the fitting and forecasting phases, the combined mean absolute percentage error (CMAPE) is used. Notably, the CMAPE can be applied as a criterion to determine the optimal time breakpoint (the time with the lowest CMAPE is selected as the optimal breakpoint). The CMAPE will also be used as a criterion for the final choice of model. The model with the lowest CMAPE is used to forecast future CO_2 emissions in BRICS countries.

$$CMAPE = \frac{1}{n+f}\sum_{k=1}^{n+f}\left|\frac{x^{(0)}(k)-\hat{x}^{(0)}(k)}{x^{(0)}(k)}\right| \times 100\% \tag{34}$$

Modelling process

To clearly show the modelling and parameter solution processes, the modelling process is depicted in the Fig. 1.

Validation of the grey breakpoint prediction models

To verify the validity and applicability of the grey breakpoint forecasting models, carbon emission data from BRICS countries are selected for analysis in this paper, and traditional grey models (GM) [68], fractional order grey models (FGM) [69], and GBPM and OGBPM models are selected for comparison. CO_2 emissions data from 2009–2019 are used for modelling, and CO_2 emissions data from 2020–2021 are applied for projection comparison. The CO_2 emissions data are obtained from the BP Statistical Review of World Energy. Overall, seven grey projection models are constructed to predict two periods backward. The breakpoint and fuzzy breakpoint intervals are set according to each country's carbon emission policies and the available raw data, and the parameter estimates, fitted values and predicted values of each model are calculated. Finally, the MAPE and FMAPE of the seven models are compared, and the model with the smallest combined error is selected as the optimal prediction model.

The CO_2 emissions of Brazil

Figure 2 shows that before 2014, Brazil's CO_2 emissions displayed an upwards trend, likely influenced by environmental protection policies, and after 2014, CO_2 emissions showed a downwards trend; therefore, 2014, i.e., $t^* = 6$, is selected as the breakpoint of the GBPM and OGBPM models. Then, the GM and FGM methods are used to establish four benchmark models, and the prediction error is calculated.

Since the impact of environmental policies on CO_2 emissions is continuous, 2012–2016 is selected as the fuzzy breakpoint interval for the NOGBPM, NGBPM, and AGBPM models, i.e., $t = (5, 6, 7, 8)$; then, by calculating the CMAPE of the three models at different times, the optimal breakpoints of the three models are determined according to the minimum CMAPE as $t_m = 7$, $t_m = 4$, and $t_m = 8$, and optimal predictions are obtained. The process of background value optimisation using PSO is shown in Fig. 3. The specific parameters of each model are shown in Table 1, and the seven sets of predicted values are shown in Fig. 4.

The fit of the GM is a slowly rising straight line, and the fit of the FGM is a smooth curve that rises and then

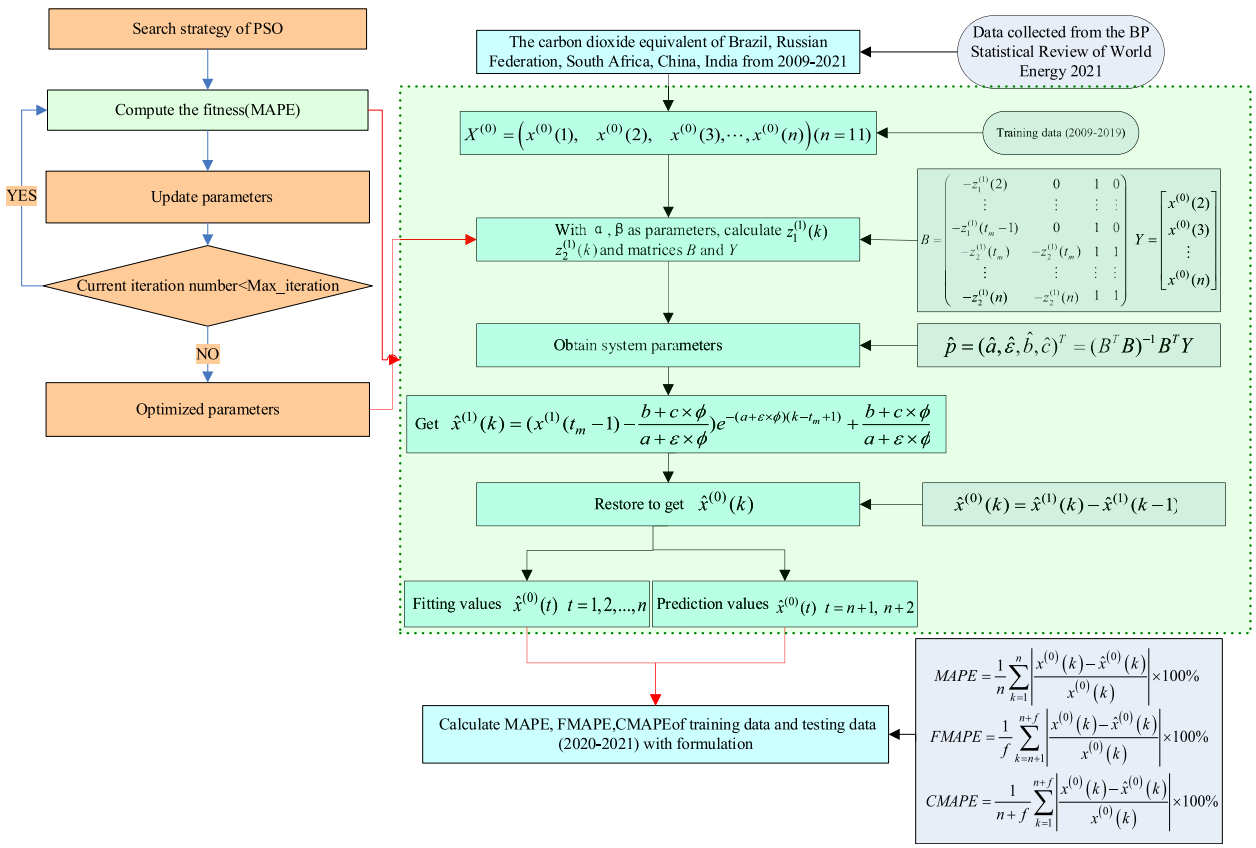

Fig. 1 Flow chart of modelling

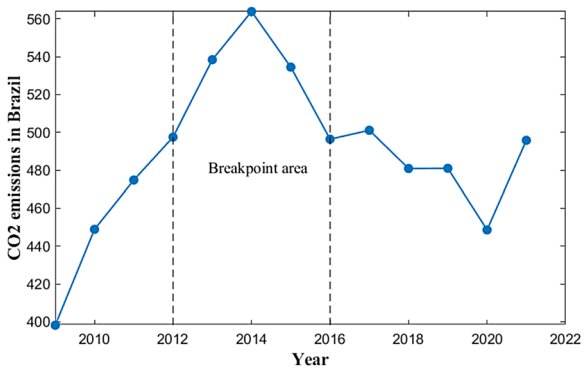

Fig. 2 CO_2 emissions in Brazil from 2009–2021

falls. The coefficient of mutation c for the GBPM is much smaller than 0, which is equivalent to shifting the fitted curve significantly downwards at the breakpoint. The coefficient of change in development ε for both the OGBPM and NOGBPM models is greater than 0, and $|\varepsilon| > a$, which corresponds to a change in the direction of the fitted data at the breakpoint. The coefficient of mutation c for the NGBPM is greater than 0 but generally small, which is equivalent to shifting the fitted curve upwards by some distance. The coefficient of mutation c and coefficient of change in development ε for the AGBPM have different signs, reflecting the trends of the fitted data before and after the breakpoint. These results illustrate that the model with temporal breakpoints yields the best fit and that the optimised model best depicts the trends in the original data.

A comparison of the errors of the seven models is shown in Table 2 and Fig. 5. During the simulation phase, the MAPE values of both the OGBPM and the NOGBPM are relatively small. However, the OGBPM is affected by overfitting, mainly due to the characteristics of the model, which equates to constructing distinct GM(1,1) models for the periods preceding and succeeding a temporal breakpoint t^*; thus, the corresponding fitted data are split before and after a breakpoint,

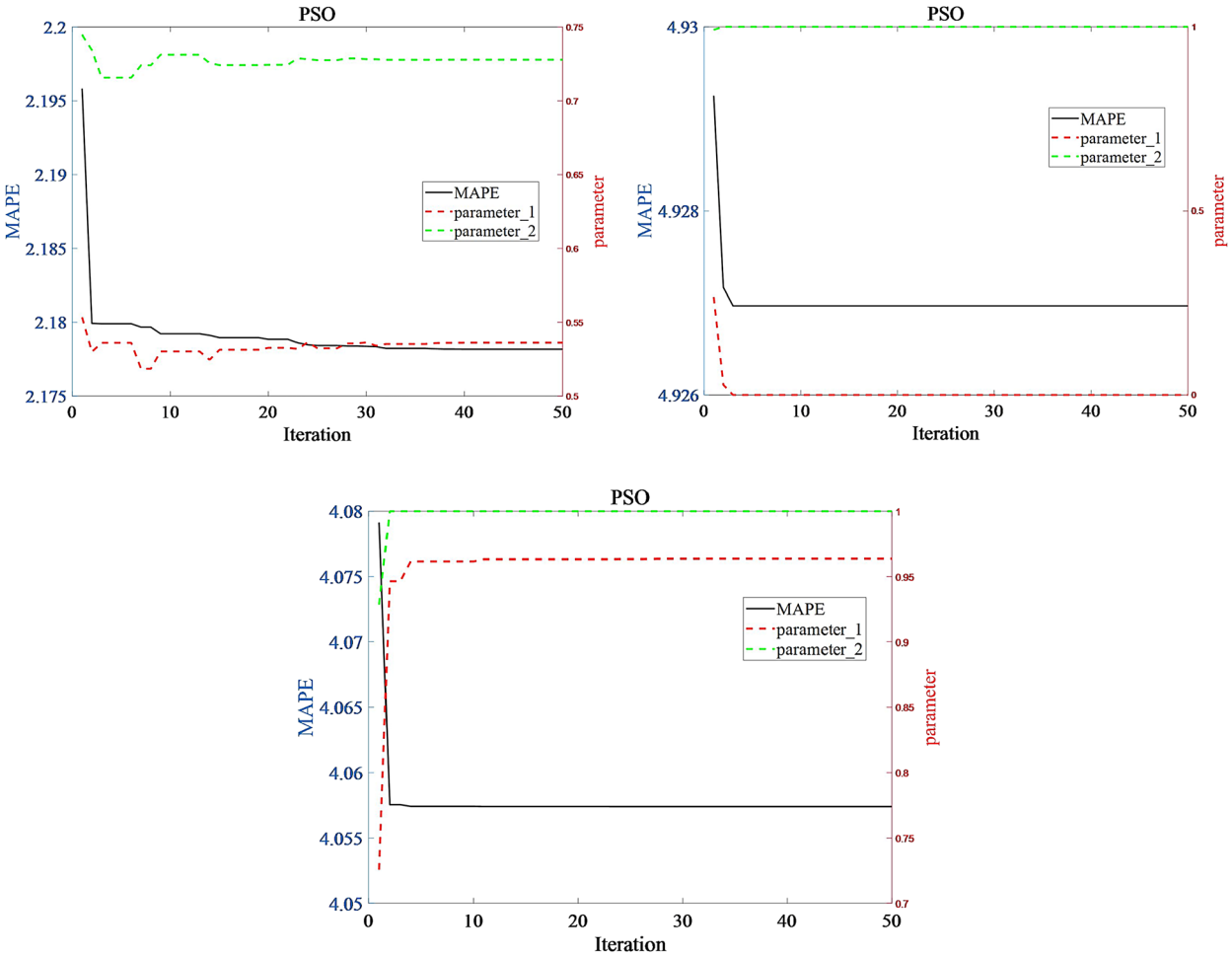

Fig. 3 PSO process for background value coefficients

Table 1 Coefficient estimates

Model	Coefficient estimates
GM	$a = -0.0022$, $b = 495.2651$
FGM	$r = 0.6155$, $a = 0.0644$, $b = 378.6288$
GBPM	$t = 6$, $a = -0.0597$, $b = 409.7168$, $c = -135.2210$
OGBPM	$t = 6$, a $= -0.0597$, $b = 409.7168$, $\varepsilon = 0.0922$, $c = 227.7881$
NOGBPM	$t = 7$, $a = -0.0581$, $b = 410.4514$, $\varepsilon = 0.0830$, $c = 195.4888$, $a = 0.5366$, $\beta = 0.7270$
NGBPM	$t = 4$, $a = 0$, $\beta = 1$, $a = 0.0061$, $b = 463.0535$, $c = 54.0779$,
AGBPM	$t = 8$, $a = -0.0339$, $b = 440.5392$, $\varepsilon = 0.0259$, $a = 0.9646$, $\beta = 1$

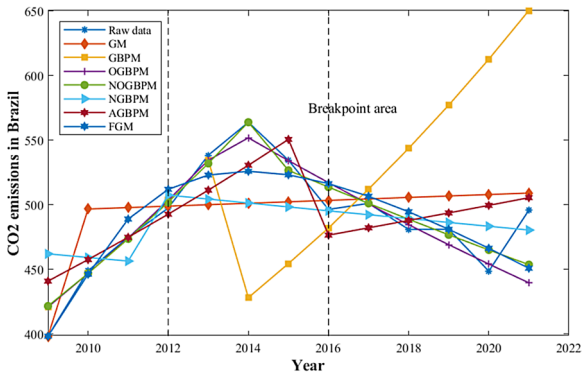

Fig. 4 Simulation and prediction of CO_2 emissions in Brazil from 2009–2021

which is also equivalent to creating two different fitted curves that are spliced together. This approach leads to a very small MAPE and consequently a small CMAPE. The original data before the breakpoint are not fully utilised in predictions, and the amount of data after the breakpoint is often limited, making it difficult to guarantee forecasting accuracy. In the forecasting stage, the NOGBPM yields the smallest FMAPE and demonstrates the highest precision in forecasting. Therefore, from the above analysis of the fitting curves and modelling error, it can be concluded that the NOGBPM offers the highest fitting degree and most accurate predictive performance for CO_2 emissions in Brazilian. Notably, this model can simulate the real system trends and accurately predict future data. Therefore, the NOGBPM is finally chosen to forecast CO_2 emissions in Brazil from 2022 to 2025.

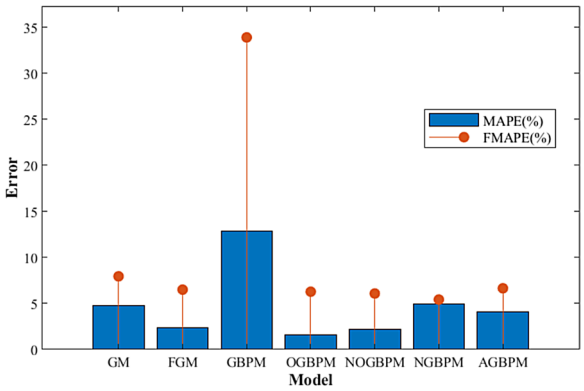

Fig. 5 Simulation and prediction errors for CO_2 emissions in Brazil

The CO_2 emissions of Russia

Figure 6 shows that Russia's CO_2 emissions change in approximately 2011 and approximately 2015, and the change is greater in 2015; therefore, 2015, i.e., $t^* = 7$, is selected as the breakpoint for the GBPM and OGBPM models. Then, the GM and FGM methods are used to establish four benchmark models, and the modelling errors are calculated.

It is difficult to determine the optimal time breakpoint based on data assessment and policy analysis alone; therefore, 2011–2015 is selected as the fuzzy breakpoint interval for the NOGBPM, NGBPM and AGBPM models, i.e., $t = (3, 4, 5, 6, 7)$. Then, the optimal breakpoints for the three models are determined by calculating the CMAPE values at different times. The optimal breakpoints of the three models are $t_m = 5$, $t_m = 3$, and $t_m = 3$ according to the minimum CMAPEs, and optimal forecasts are obtained. The process of background value optimisation using PSO is shown in Fig. 7. The specific parameters of each model are shown in Table 3, and the seven sets of predicted values are shown in Fig. 8.

Since the optimal cumulative order of the FGM is 1, the fitted results of the FGM and GM models overlap as a slowly rising straight line, which does not fit the trend of the data very well. The GBPM and the OGBPM overlap before the breakpoint, and after the breakpoint, the coefficient of mutation c is less than 0 in both cases, reflecting a gradual reduction in CO_2 emissions. The coefficient of change in development ε of the OGBPM is smaller than 0, indicating that the emissions trend accelerates after the breakpoint, which does not reflect the actual situation;

Table 2 Simulation and prediction errors for CO_2 emissions in Brazil

Error	GM	FGM	GBPM	OGBPM	NOGBPM	NGBPM	AGBPM
MAPE(%)	4.7887	2.3768	12.8554	1.6185	2.1769	4.9242	4.0559
FMAPE(%)	7.9519	6.5066	33.8892	6.2826	6.0870	5.4252	6.6495
CMAPE(%)	5.2753	3.0122	16.0914	2.3360	2.7785	5.0013	4.4549

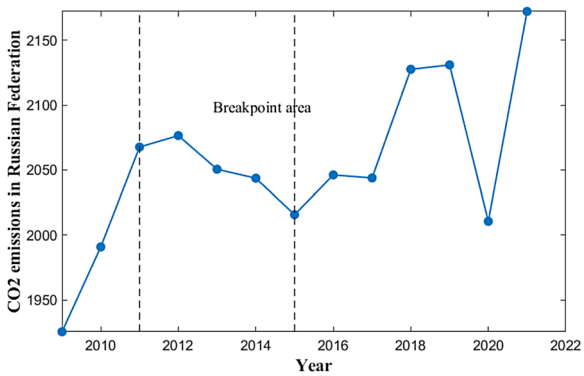

Fig. 6 CO_2 emissions in Russia from 2009–2021

additionally, the coefficient of change in development ε and the coefficient of mutation c of the NOGBPM are both larger than 0 but generally small, and the corresponding fitted curve is relatively flat. The coefficient of mutation c of the NGBPM is larger than 0 and is equivalent to shifting the fitted curve upwards by a certain distance. The coefficient of change in development ε and development coefficient a of the AGBPM have opposite signs, reflecting the trends of the fitted data before and after a breakpoint. The optimal breakpoint in the AGBPM case is the same as that for the NOGBPM model, so the parameters and fitted curves are very similar.

A comparison of the errors of the seven models is shown in Table 4 and Fig. 9. In the simulation phase, the OGBPM yields the smallest MAPE, but in reality, the OGBPM is influenced by overfitting, which in turn leads to small CMAPE values; thus, prediction accuracy is difficult to guarantee. In the prediction stage, the NOGBPM yields the smallest FMAPE and the best prediction accuracy. Therefore, the NOGBPM displays optimal performance in both the simulation and prediction stages, reflecting the superiority of the new model. From the above analysis of the fitting curves and modelling errors, it can be concluded that the NOGBPM provides the best fit and prediction accuracy; therefore, the NOGBPM is finally chosen to forecast the CO_2 emissions in Russia from 2022–2025.

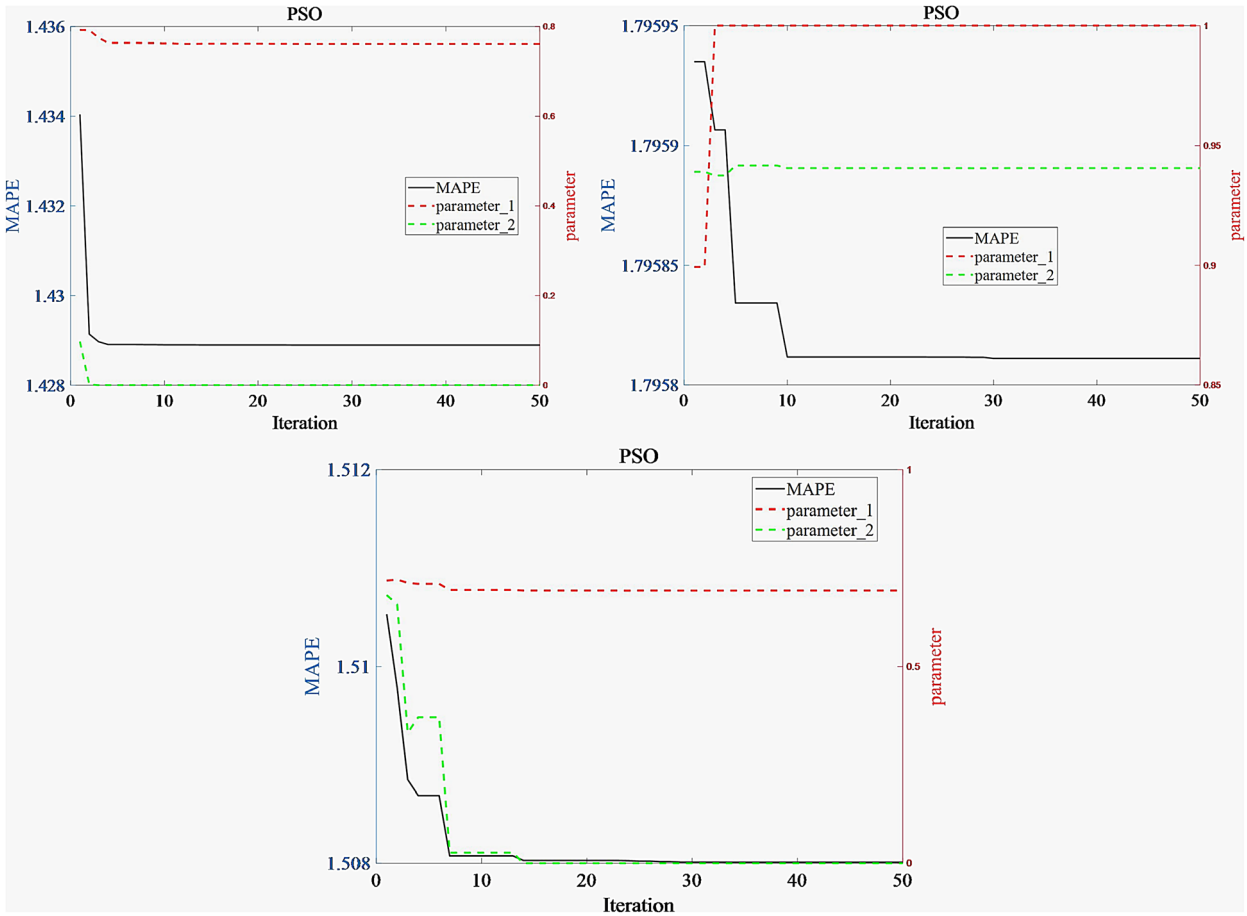

Fig. 7 PSO iterative process for background value coefficients

Table 3 Coefficient estimates

Model	Coefficient estimates
GM	$a = -0.0043$, $b = 2006.2633$
FGM	$r = 1$, $a = -0.0043$, $b = 2006.2633$
GBPM	$t = 7$, $a = -0.0042$, $b = 2015.7876$, $c = -16.8144$
OGBPM	$t = 7$, $a = -0.0042$, $b = 2015.7876$, $\varepsilon = -0.0108$, $c = -203.2097$
NOGBPM	$t = 5$, $a = -0.0207$, $b = 1931.0668$, $\varepsilon = 0.0130$, $c = 25.9718$, $a = 0.7619$, $\beta = 0$
NGBPM	$t = 3$, $a = -0.0032$, $b = 1978.1822$, $c = 43.0684$, $a = 1$, $\beta = 0.9417$
AGBPM	$t = 5$, $a = -0.0148$, $b = 1968.7888$, $\varepsilon = 0.0085$, $a = 0.6928$, $\beta = 0$

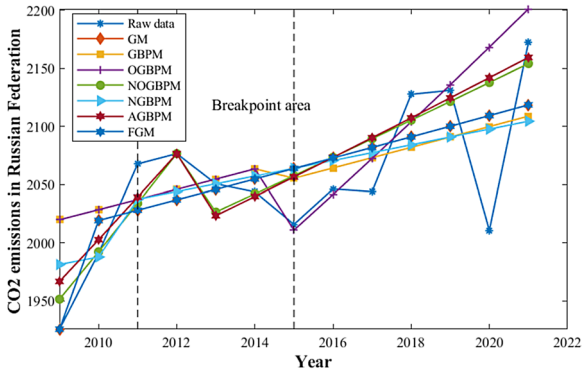

Fig. 8 Simulation and prediction of CO_2 emissions in Russia from 2009–2021

The CO_2 emissions of India

Figure 10 shows that India's CO_2 emissions have consistently displayed an upwards trend, and the nature of the breakpoint is not obvious; however, since the upwards trend decreases after 2018 and the data for 2020 indicate a decrease in emissions, $t^* = 10$ is selected as the breakpoint for the GBPM and OGBPM models. Then, the GM and FGM methods are used to establish the four benchmark models, and the corresponding modelling error is calculated.

In this case, we set 2011–2019 as the fuzzy breakpoint interval for the NOGBPM, NGBPM and AGBPM models, i.e., $t = (3, 4, 5, 6, 7, 8, 9, 10, 11)$, and then determine the optimal breakpoints for the three models by calculating the CMAPE values at different times. The optimal breakpoints of the three models are $t_m = 10$, $t_m = 3$, and $t_m = 10$ according to the minimum CMAPEs, and optimal predictions are obtained. The process of background value optimisation using PSO is shown in Fig. 11. The specific parameters are shown in Table 5, and the seven sets of predicted values are shown in Fig. 12.

The upwards trend in CO_2 emissions in India is evident, with overfitting of the fitted curves for each model before the breakpoint. After the optimal breakpoint, the fitted curves for both NOGBPM and AGBPM decrease, with more realistic fits. The errors of the seven models are compared, as shown in Table 6 and Fig. 13. During the simulation phase, the OGBPM yields the smallest MAPE, but in reality, the OGBPM is influenced by overfitting. Additionally, the GM and FGM provide better

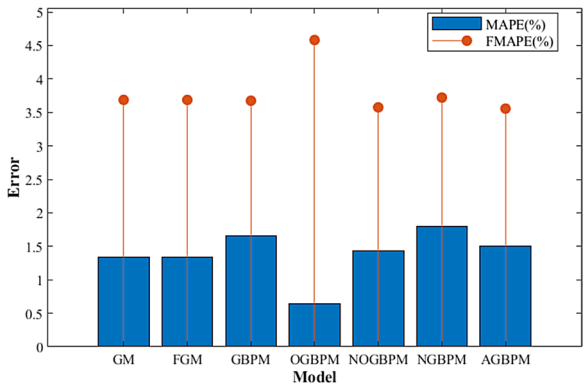

Fig. 9 Simulation and prediction errors for CO_2 emissions in Russia

Table 4 Simulation and prediction errors of CO_2 emissions in Russia

Error	GM	FGM	GBPM	OGBPM	NOGBPM	NGBPM	AGBPM
MAPE(%)	1.3385	1.3385	1.6605	0.6426	1.4284	1.7955	1.5076
FMAPE(%)	3.6874	3.6874	3.6753	4.5816	3.5755	3.7219	3.5575
CMAPE(%)	1.6999	1.6999	1.9705	1.2486	1.7587	2.0919	1.8230

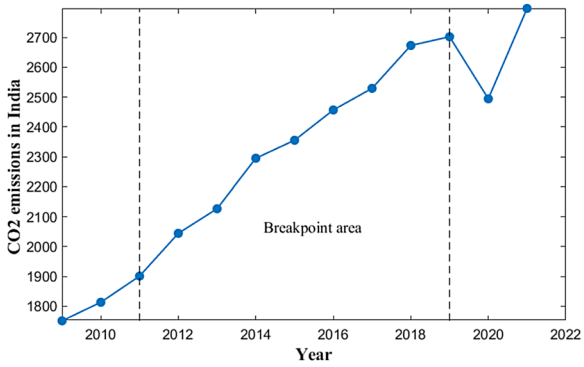

Fig. 10 CO_2 emissions in India from 2009–2021

data fitting results with stable trends, and the NOGBPM yields MAPE < 2%, which reflects a good fit. In the projection stage, the abrupt changes in the raw data in 2020 lead to large values of the overall FMAPE; however, due to the poor selection of breakpoints with the OGBPM and NOGBPM models, the NOGBPM performs best, with a forecasting error of only 5.4% and a combined error of only 2.2%. In summary, the NOGBPM yields the best modelling accuracy and forecasting performance for CO_2 emission in India and is selected to forecast India's CO_2 emissions from 2022–2025.

The CO_2 emissions of China

Figure 14 shows that China's CO_2 emissions gradually decreased from 2011 to 2015, but it is difficult to determine the optimal breakpoint through manual observation of the data; therefore, 2011–2015 is selected as the fuzzy breakpoint interval for the NOGBPM, NGBPM and AGBPM models, i.e. $t = (3, 4, 5, 6, 7)$, and the optimal breakpoints for the three models are determined by calculating the CMAPE values at different times. The optimal breakpoints of the three models are $t_m = 7$, $t_m = 3$, and $t_m = 7$ according to the minimum CMAPE values, and the optimal predictions are obtained. The process of background value optimisation using PSO is shown in Fig. 15. Among the above three models, two yield the best results at $t_m = 7$; therefore, $t^* = 7$ is set as the

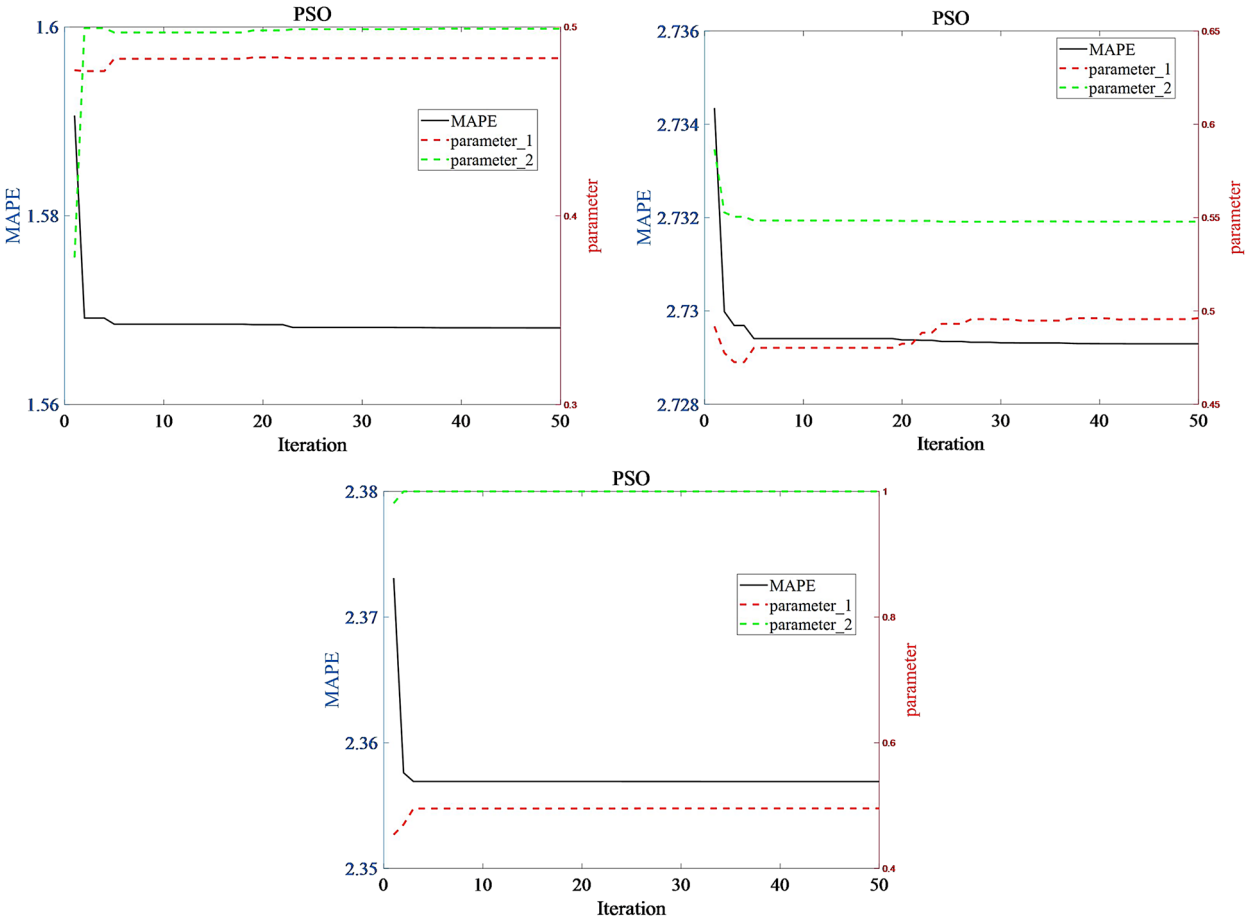

Fig. 11 PSO iterative process for background value coefficients

Table 5 Coefficient estimates

Model	Coefficient estimates
GM	$a = -0.0442$, $b = 1743.1920$
FGM	$r = 0.8975$, $a = -0.0270$, $b = 1610.2394$
GBPM	$t = 10$, $a = -0.0479$, $b = 1712.8329$, $c = -77.5731$
OGBPM	$t = 10$, $a = -0.0479$, $b = 1712.8329$, $c = 735.5023$, $\varepsilon = 0.0370$
NOGBPM	$t = 10$, $a = -0.0479$, $b = 1714.2486$, $c = 734.2379$, $\varepsilon = 0.0371$, $a = 0.4830$, $\beta = 0.4990$
NGBPM	$t = 3$, $a = -0.0426$, $b = 1700.1889$, $c = 65.4274$, $a = 0.4964$, $\beta = 0.5476$
AGBPM	$t = 10$, $a = -0.0477$, $b = 1716.2077$, $\varepsilon = 0.0061$, $a = 0.4950$, $\beta = 1$

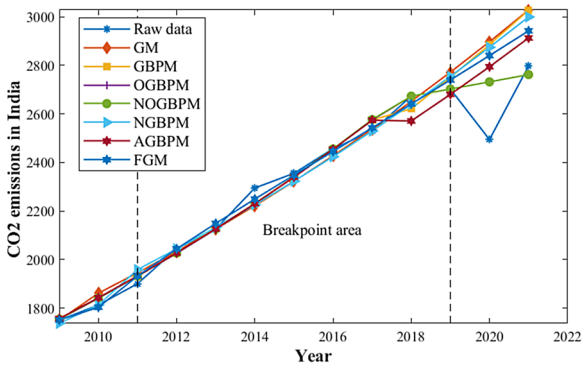

Fig. 12 Simulation and prediction of CO_2 emissions in India from 2009–2021

breakpoint for the GBPM and OGBPM models. Next, the GM and FGM methods are used to establish benchmark models, and the modelling errors are calculated. The specific parameters are shown in Table 7, and the seven sets of predicted values are shown in Fig. 16.

The fit for the GM results in a straight line with an upwards trend, the fit for the FGM results in a smooth curve that rises and then falls, and the models with a breakpoint set to 7 all show some degree of a downwards trend after the breakpoint, which reflects the actual situation. For the OGBPM, NOGBPM and AGBPM models, the coefficient of change in development ε and the development coefficient a have different signs, indicating that the trend of the fitted data after the breakpoint

Table 6 Simulation and prediction errors for CO_2 emissions in India

Error	GM	FGM	GBPM	OGBPM	NOGBPM	NGBPM	AGBPM
MAPE (%)	1.3679	0.8259	1.8503	1.0766	1.5679	2.7288	2.3566
FMAPE (%)	12.1953	9.5150	11.9448	5.3948	5.3953	11.2262	8.0717
CMAPE (%)	3.0336	2.1626	3.4033	1.7409	2.1567	4.0361	3.2358

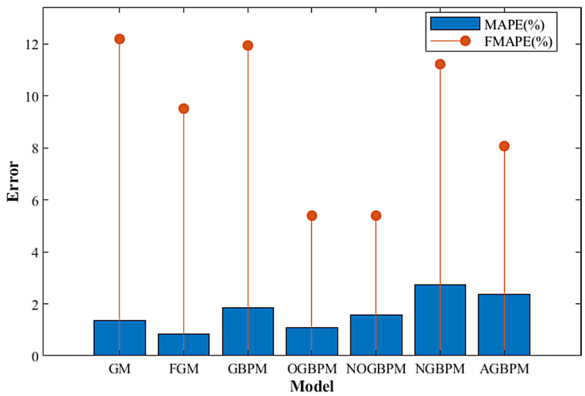

Fig. 13 Simulation and prediction errors for CO_2 emissions in India

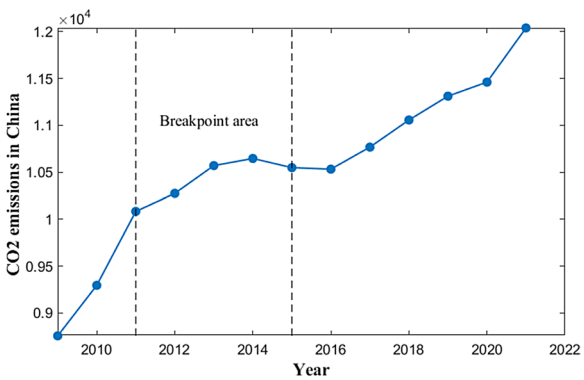

Fig. 14 CO_2 emissions in China from 2009–2021

has slowed. An error comparison of the seven models is shown in Table 8 and Fig. 17. In the simulation stage, all seven models display good modelling performance, but the OGBPM is influenced by overfitting, and the AGBPM performs best among the three new models proposed in this paper. In the prediction stage, the AGBPM displays the best prediction accuracy and can reflect the real system changes for the accurate prediction of future data. Therefore, the AGBPM is finally chosen to forecast China's CO_2 emissions from 2022 to 2025.

The CO_2 emissions of South Africa

Figure 18 shows that the trend of CO_2 emissions in South Africa is very complex, and it is difficult to determine the

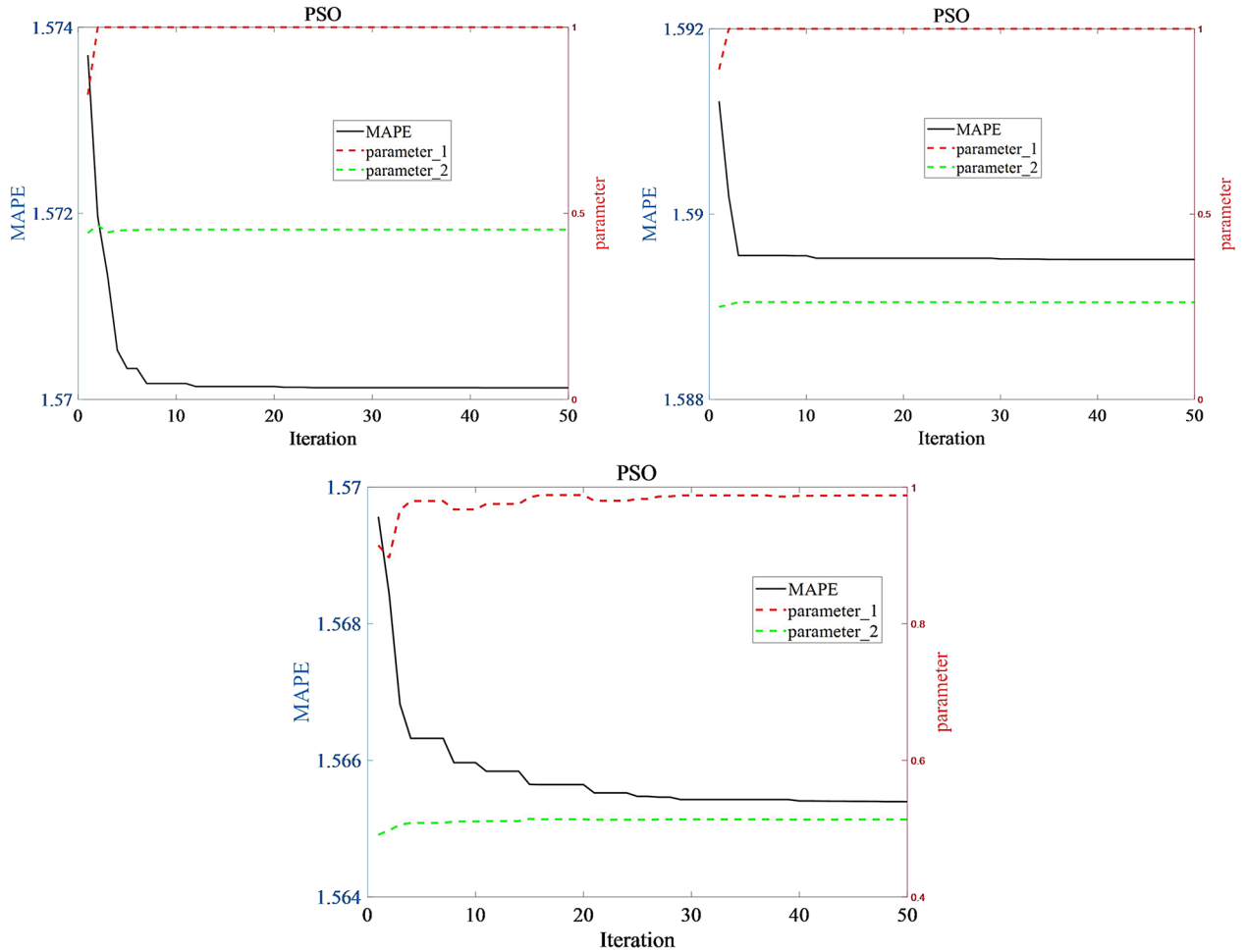

Fig. 15 PSO iteration process for background value coefficients

Table 7 Coefficient estimates

Model	Coefficient estimates
GM	$a = -0.0155$, $b = 9574.3042$
FGM	$r = 0.8312$, $a = 0.0143$, $b = 8517.5448$
GBPM	$t = 7$, $a = -0.0309$, $b = 9135.5219$, $c = -962.6042$
OGBPM	$t = 7$, $a = -0.0309$, $b = 9135.5219$, $c = 65.5797$, $\varepsilon = 0.0119$
NOGBPM	$t = 7$, $a = -0.0305$, $b = 8993.4245$, $c = 215.3964$, $\varepsilon = 0.0115$, $\alpha = 1$, $\beta = 0.4561$
NGBPM	$t = 3$, $a = -0.0119$, $b = 9079.9911$, $c = 819.7682$, $\alpha = 1$, $\beta = 0.2619$
AGBPM	$t = 7$, $a = -0.0297$, $b = 9035.6664$, $\varepsilon = 0.0088$, $\alpha = 0.9881$, $\beta = 0.5133$

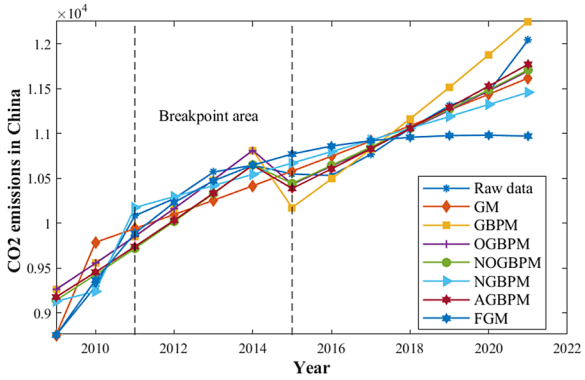

Fig. 16 Simulation and prediction of CO_2 emissions in China from 2009–2021

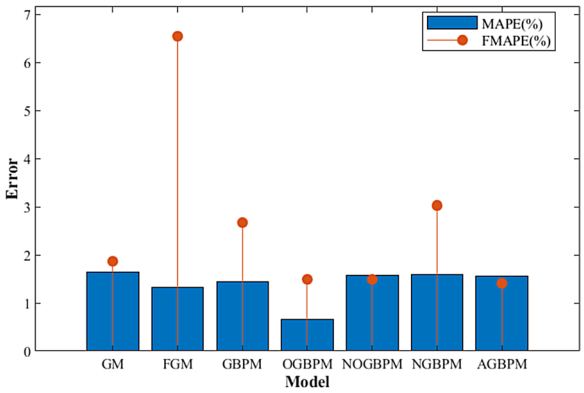

Fig. 17 Simulation and prediction errors for CO_2 emissions in China

optimal breakpoint based on observation alone. Therefore, 2012–2019 is selected as the fuzzybreakpoint interval of the NOGBPM, NGBPM, and AGBPM models, i.e., $t = (3, 4, 5, 6, 7, 8, 9, 10, 11)$, and the optimal breakpoints of the three models are determined by calculating the CMAPE at different times. The optimal breakpoints of the three models are $t_m = 8$, $t_m = 6$, and $t_m = 6$ according to the minimum CMAPE values, and the optimal predictions are obtained. The process of background value optimisation using PSO is shown in Fig. 19. Among the above three models, two of them both yield the best results at $t_m = 6$, so $t^* = 6$ is selected as the breakpoint for the GBPM and OGBPM models. Then, GM and FGM baseline models are established, and the modelling errors are calculated. The specific parameters are shown in Table 9, and the seven sets of predicted values are shown in Fig. 20.

Since the optimal cumulative order of the FGM is 1, the fitted results of the FGM and GM models overlap as a slowly declining straight line, which does not fit the trend of CO_2 emissions well. The results of the GBPM and OGBPM overlap before the breakpoint and display a downwards trend, and at the breakpoint, the GBPM result shifts substantially upwards, but the trend is still downwards. Additionally, the ε value of the OGBPM is less than 0, and $|\varepsilon| > a$, indicating an upwards trend in the fitted data after the breakpoint and reflecting a gradual increase in CO_2 emissions; these results reflect the sudden increases in emissions in 2016 and 2019. The ε

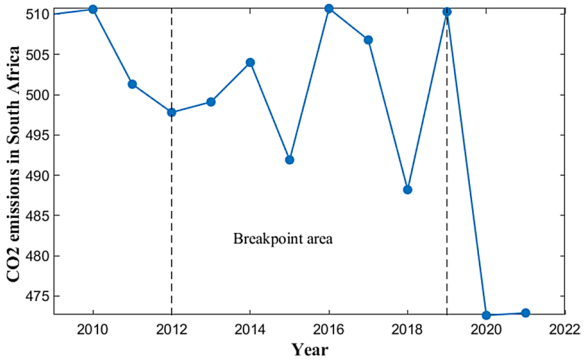

Fig. 18 CO_2 emissions in South Africa from 2009–2021

and c values of the NOGBPM, NGBPM and AGBPM models are small, and all these models fit the original data well, with NGBPM being the most accurate in 2020 and 2021, reflecting its excellent forecasting performance.

A comparison of the errors of the seven models is shown in Table 10 and Fig. 21. In the simulation stage, the GM and FGM models yield the smallest MAPE, but in practice, there is not much difference between the models. In the prediction stage, the NGBPM produces the smallest FMAPE and optimal prediction accuracy, while the GM and FGM models yield the largest FMAPE values. Although the final combined error of 1.9245% for the GM and FGM models is smaller than that of 1.9265% for the NGBPM model, based on the

Table 8 Simulation and prediction errors for CO_2 emissions in China

Error	GM	FGM	GBPM	OGBPM	NOGBPM	NGBPM	AGBPM
MAPE (%)	1.6355	1.3233	1.4367	0.6542	1.5701	1.5894	1.5654
FMAPE (%)	1.8665	6.5404	2.6713	1.4907	1.4912	3.0247	1.4083
CMAPE (%)	1.6710	2.1259	1.6266	0.7829	1.5580	1.8102	1.5412

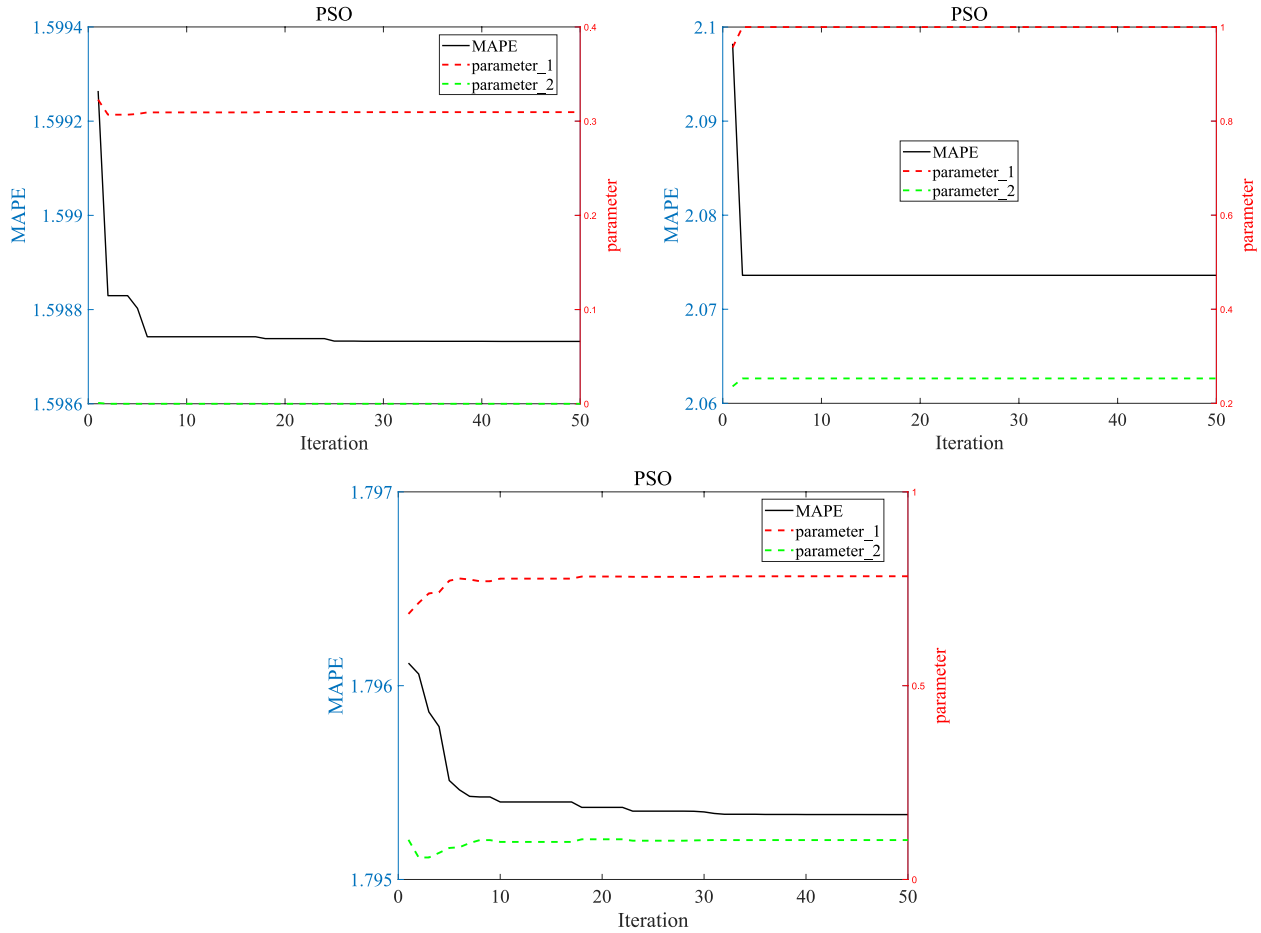

Fig. 19 PSO iteration process for value coefficients

Table 9 Coefficient estimates

Model	Coefficient estimates
GM	$a = 0.0003$, $b = 503.0479$
FGM	$r = 1$, $a = 0.0003$, $b = 503.0479$
GBPM	$t = 6$, $a = 0.0075$, $b = 513.7434$, $c = 18.8120$
OGBPM	$t = 6$, $a = 0.0075$, $b = 513.7434$, $c = -15.5447$, $\varepsilon = -0.0085$
NOGBPM	$t = 8$, $a = 0.0048$, $b = 510.0705$; $c = 11.3591$, $\varepsilon = -0.0007$, $a = 0.3168$, $\beta = 0$
NGBPM	$t = 6$, $a = 0.0040$; $b = 503.2481$; $c = -1.2596$; $a = 1$; $\beta = 0.3449$
AGBPM	$t = 6$, $a = 0.0040$; $b = 508.1228$; $\varepsilon = -0.0025$; $a = 0.7880$; $\beta = 0.0885$

above fitting curve and error analysis, it is obvious that the NGBPM is most suitable; therefore, the NGBPM is selected to forecast South Africa's CO_2 emissions from 2022 to 2025.

In the comprehensive analysis of the performance of the seven models described above for forecasting CO_2 emissions in BRICS countries, the GM and the FGM produce smooth curves; therefore, these models cannot capture the trend of CO_2 emissions data or provide accurate system forecasts after an external shock to the system. Compared with the GM and FGM models, the three grey breakpoint prediction models are capable of accurately capturing the actual variations within the system, but the original breakpoint models, the GBPM

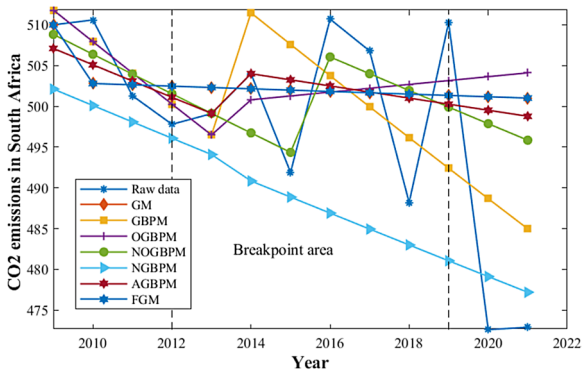

Fig. 20 Simulation and prediction of CO_2 emissions in South Africa from 2009–2021

and OGBPM, set unique breakpoints. Thus, the optimal breakpoint cannot be easily confirmed if the data trend is complex. The NOGBPM, NGBPM and AGBPM models use fuzzy breakpoint intervals to achieve accurate system predictions. The NOGBPM performs best in fitting data for Brazil, Russia and India, the AGBPM performs best in fitting data for China and the NGBPM performs best in fitting data for South Africa.

Application in forecasting the CO_2 emissions of BRICS countries

In this section, the CO_2 emissions of BRICS countries are forecasted from 2022–2025. Based on the analytical findings from the preceding discussion, the optimal forecasting models and optimal breakpoints are selected, and the parameters are calculated as presented in Table 11, where c of the AGBPM used for China and ε of the NGBPM used for South Africa are both null values. The development coefficient a and grey action b in Brazil were −0.058 and 410.774 before the breakpoint respectively, which changed to 0.017 and 568.634 after the breakpoint, indicating a transition from an increasing to a decreasing trend in the fitted values of CO_2 emissions in Brazil. The development coefficient a and grey action b in Russia were − 0.021 and 1931.111 before the breakpoint respectively, which changed to 0.007 and 1979.598 after the breakpoint, suggesting a slowdown in the growth trend of the fitted values of CO_2 emissions in Russia. The development coefficient a and grey action b in India were − 0.048 and 1714.248 before the breakpoint respectively, which shifted to − 0.006 and 2535.500 after the breakpoint, indicating a significant slowdown in the growth trend of the fitted values of CO_2 emissions in India. The development coefficient a in China was − 0.033 before the breakpoint, which shifted to − 0.020 after the breakpoint, suggesting a slowdown in the growth trend of the fitted values of CO_2 emissions in China. The grey action b in South Africa was 503.248 before the breakpoint and decreased to 494.678 after the breakpoint, indicating a further expansion of the decreasing trend in the fitted values of CO_2 emissions in South Africa.

As presented in Table 12 and Fig. 22, the projections show that from 2022 to 2025, CO_2 emissions in Brazil and South Africa will decrease annually by 6.47% and 1.6%, with average annual rates of decrease of 1.68% and 0.40%, respectively. In contrast, CO_2 emissions in Russia, India and China will increase annually by 2.28%, 2.28% and 8.38%, with annual growth rates of 0.56%, 0.57% and 2.03%, respectively. The differences in CO_2 emissions trends among the BRICS countries mainly stem from significant divergences in their development paths and energy structures: Brazil has achieved deep emission reductions through the large-scale application of biofuels and a clean energy structure dominated by hydropower, complemented by rainforest protection policies that enhance its carbon sink capacity. Russia's oil and gas export-oriented economy has driven CO_2 emissions

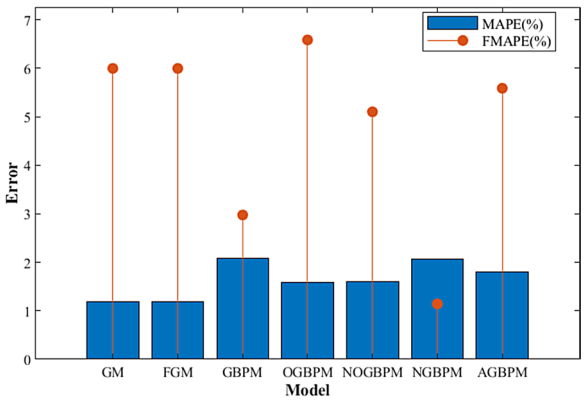

Fig. 21 Simulation and prediction errors for CO_2 emissions in South Africa

Table 10 Simulation and prediction errors for CO_2 emissions in South Africa

Error	GM	FGM	GBPM	OGBPM	NOGBPM	NGBPM	AGBPM
MAPE (%)	1.1843	1.1843	2.0873	1.5940	1.5992	2.0688	1.7952
FMAPE (%)	5.9959	5.9959	2.9775	6.5838	5.1007	1.1436	5.5860
CMAPE (%)	1.9245	1.9245	2.2242	2.3616	2.1379	1.9265	2.3784

Table 11 Model selection and parameter estimation

Country	Model	*t*	*a*	*b*	*c*	*ε*	*α*	*β*	MAPE (%)
Brazil	NOGBPM	7	− 0.0580	410.7741	157.8596	0.0750	0.5366	0.3082	2.1755
Russia	NOGBPM	5	− 0.0207	1931.1110	48.4874	0.0151	0.7619	0.0000	1.4638
India	NOGBPM	10	− 0.0480	1714.2483	821.2520	0.0423	0.4830	0.0000	1.7543
China	AGBPM	7	− 0.0333	9105.6289	–	0.0132	0.3117	0.7061	1.5060
South Africa	NGBPM	6	0.0040	503.2481	− 8.5702	–	1.0000	0.3195	2.6125

upward, but the export of nuclear energy technology and an increase in the share of nuclear energy have partially mitigated carbon growth. As the global manufacturing hub, China's coal-dominated energy structure and rapid urbanization process have propelled continuous growth in CO_2 emissions; however, with the intensification of emission reduction policies, China has made substantial investments in photovoltaic and wind power, and more advanced energy infrastructure and clean technology innovations have effectively reduced carbon intensity. India similarly faces emission pressures stemming from its reliance on coal-fired power and accelerated industrialization, leading to a"carbon lock-in effect,"although the expansion of renewable energy has partially alleviated the growth rate. South Africa, relying on the accelerated replacement of coal-fired power with renewable energy and the implementation of carbon tax policies, has seen relatively moderate reductions due to the inertia of its coal-fired power infrastructure and lagging industrial transformation. These differences are essentially the result of a combination of countries'resource endowments, industrial policies, and technological innovation capabilities.

Conclusion

In this paper, the concept of temporal breakpoints is introduced into grey models, and three new grey breakpoint forecasting models based on the GM(1,1), GBPM(1,1,t) and OGBPM(1,1,t) models are established: the NOGBPM(1,1,t) with shocks acting on both the development coefficient *a* and the grey action *b*, the NGBPM(1,1,t) with shocks acting only on the grey action *b*, and the AGBPM(1,1,t) with shocks acting only on the development coefficient *a*. These three models consider external disturbances, use fuzzy time breakpoints to account for the effects of changes in external shocks on the system, include unified methods for parameter estimation and the establishment of time response equations, and optimise the background values before and after breakpoints separately based on PSO. Second, to verify the effectiveness of the three grey breakpoint forecasting models, GM, FGM, GBPM and OGBPM are selected for comparison to simulate and forecast the carbon emission data in five BRICS countries. Based on the original data trends and policy analysis, time breakpoints and fuzzy breakpoint intervals are set, the optimal time breakpoints, parameter estimates, fitted values and predicted values of each model are obtained, and the prediction performance of the seven models is compared. Finally, the model with the lowest combined error is selected as the optimal prediction model, and the optimal time breakpoints are identified. The CO_2 emissions of the BRICS countries are predicted for the period of 2022–2025. The main conclusions are as follows.

First, the introduction of time breakpoints into the grey model, including the utilization of time breakpoints and fuzzy breakpoint intervals, is applied to segregate the system into two distinct segments before and after a change, thus improving the ability to fit data, especially for

Table 12 Projected CO_2 emissions in BRICS countries

Country	2021	2022	2023	2024	2025	2021–2025	2021–2025 Average annual growth rate
Brazil	464.7652	457.3116	449.6382	442.0935	434.6754	− 6.47%	− 1.68%
Russia	2124.2891	2136.2880	2148.3547	2160.4896	2172.6930	2.28%	0.56%
India	2696.9682	2712.2274	2727.5729	2743.0052	2758.5248	2.28%	0.57%
China	11,744.0751	11,982.6640	12,226.1000	12,474.4815	12,727.9091	8.38%	2.03%
South Africa	470.0959	468.2048	466.3213	464.4453	462.5770	− 1.60%	− 0.40%

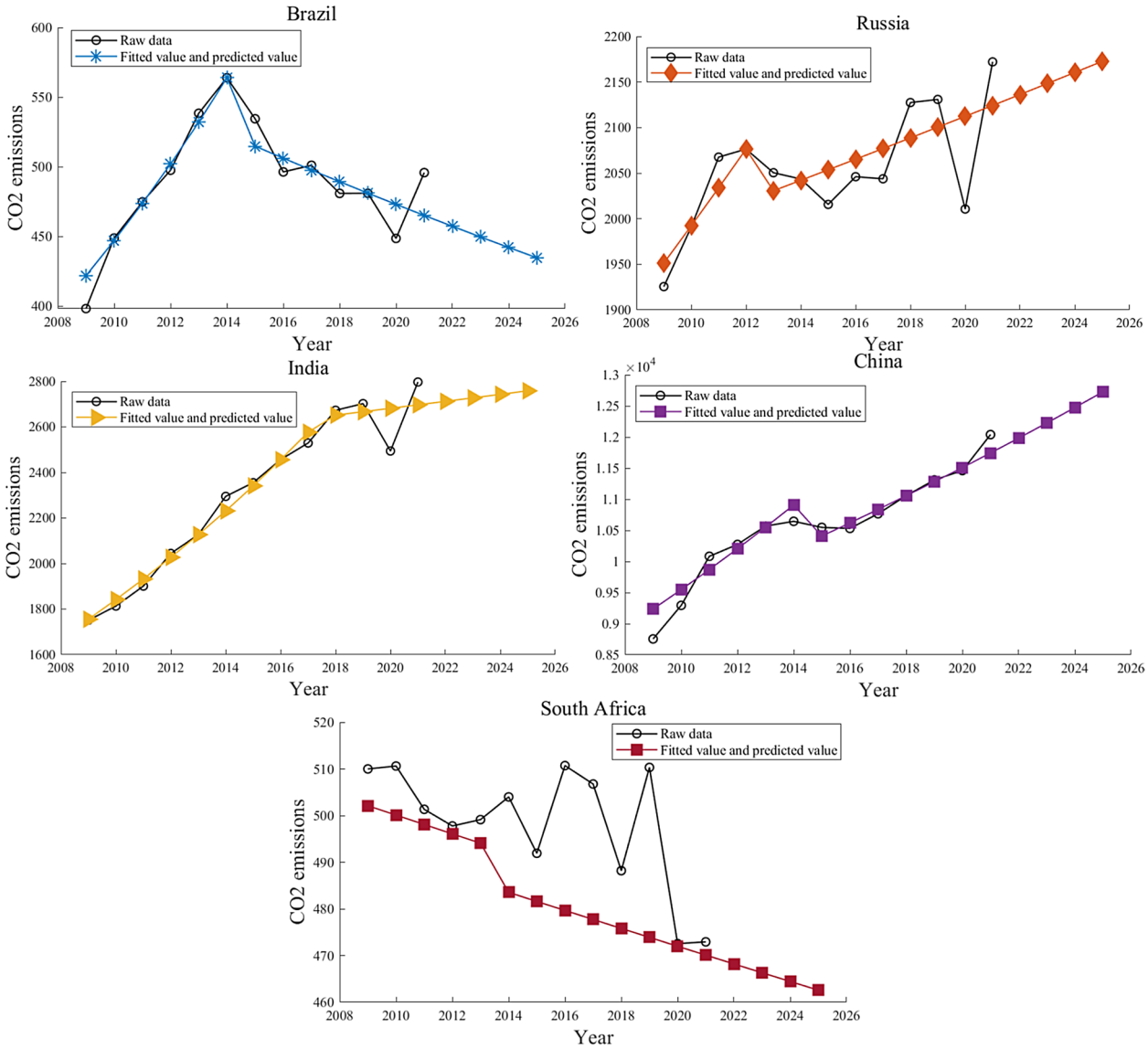

Fig. 22 Projected CO_2 emissions in BRICS countries from 2022–2025

systems with complex trends due to shocks from external factors.

Second, the fitting and forecasting results show that the three new grey breakpoint forecasting models are more efficient and accurate than the GM(1,1), FGM(1,1), GBPM (1,1,t), and OGBPM(1,1,t) models. Of these, the NOGBPM(1,1,t) performs best in fitting data for Brazil, Russia and India, the NGBPM(1,1,t) is best for South Africa and the AGBPM(1,1,t) is best for China.

Third, by 2025, the CO_2 emissions (million tons) of Brazil, Russia, India, China and South Africa will be 434.6754, 2172.693, 2758.5248, 12,727.9091 and 462.577, respectively. From 2022 to 2025, CO_2 emissions in South Africa and Brazil will decrease annually, with annual rates of decline of 1.68% and 0.40%, respectively; CO_2 emissions in Russia, India and China will increase year by year, with annual growth rates of 0.56%, 0.57% and 2.03%, respectively.

Based on the disparities in CO_2 emission trends and the potential for collaboration among BRICS countries, this study proposes the establishment of a collaborative governance framework from the following dimensions: Firstly, differentiated pathways for clean energy transitions should be formulated in accordance with the resource endowments of individual countries, with

a focus on enhancing the sharing of renewable energy technologies and integrating low-carbon industrial chains. Secondly, a multilateral green financing platform should be established by leveraging the New Development Bank to promote the interconnection of carbon markets and cross-border carbon credit offset mechanisms, while exploring the application of local currency settlements in green investments. Thirdly, joint efforts should be made to tackle key technologies such as photovoltaics, nuclear energy, and Carbon Capture, Utilization, and Storage (CCUS), and to develop a digital carbon monitoring and policy simulation system, thereby facilitating the commercialization of technological achievements and the sharing of intellectual property rights. Fourthly, a high-level dialogue mechanism for climate governance should be established to dynamically adjust Nationally Determined Contributions (NDCs) targets, pilot carbon border adjustment regulations, and promote mutual recognition of Environmental, Social, and Governance (ESG) standards, as well as the harmonization of transition finance classifications. Lastly, it should also leverage the BRICS countries as a platform to forge consensus among developing nations, restructure international energy pricing power and the discourse system in climate negotiations, and drive reforms in the global supply mechanisms for green public goods.

Based on the analysis of the above examples, the grey breakpoint prediction models can be used not only for the prediction of data with obvious breakpoint characteristics but also for the prediction of data with less obvious development trends, such as in the prediction of various systems in the post-epidemic era and the prediction of the trends of various systems under the implementation of relevant policies. Overall, these new models display strong adaptability. In addition, as this paper is based on the traditional GM(1,1) model, it is only a simple linear model. It may be possible to introduce time breakpoints into other nonlinear grey models, and their effectiveness and adaptability can be evaluated.

Abbreviations

CGE	Computable general equilibrium
IPAT	Impact-population-affluence-technology
STIRPAT	Stochastic impacts by regression on population, affluence, and technology
LEAP	Long-range energy alternatives planning system
ANN	Artificial neural network
ARIMA	Autoregressive integrated moving average
1-AGO	First-order cumulative generation operator
GM(1,1)	Grey model
GBPM(1,1,t)	Grey breakpoint prediction model
FGM(1,1,r)	Fractional-order grey model
OGBPM(1,1,t)	Optimised grey breakpoint prediction model
NOGBPM(1,1,t)	New optimised grey breakpoint prediction model
NGBPM(1,1,t)	New grey breakpoint prediction model
PSO	Particle swarm optimization
MAPE	Mean absolute percentage error
CMAPE	Combined mean absolute percentage error
FMAPE	Mean absolute percentage error of prediction

Acknowledgements
This work was supported by the National Social Science Fund of China (No. 23XTJ001), the Youth Innovation Team Research Program project of Shaanxi University (No. 24 JP059), and the Graduate Innovation Fund Project of Xi'an University of Finance and Economics (23YCZ02).

Author contributions
H.W.: Conceptualization, Formal analysis, Supervision, Writing—review and editing. X.G.: Data curation, Methodology, Writing—original draft.

Funding
This work was supported by the National Social Science Fund of China (No. 23XTJ001), the Youth Innovation Team Research Program project of Shaanxi University (No. 24 JP059), and the Graduate Innovation Fund Project of Xi'an University of Finance and Economics (23YCZ02).

Data availability
No datasets were generated or analysed during the current study.

Declarations

Ethics approval and consent to participate
Not applicable.

Competing interests
The authors declare no competing interests.

Received: 8 February 2025 Accepted: 26 April 2025
Published online: 09 May 2025

References

1. Guo JL, Liu W, Tu LP, Chen Y. Forecasting carbon dioxide emissions in BRICS countries by exponential cumulative grey model. Energy Rep. 2021;7:7238–50.
2. Sun LL, Cui HJ, Ge QS. Will China achieve its 2060 carbon neutral commitment from the provincial perspective? Adv Clim Chang Res. 2022;13:169–78.
3. Nguyen HT, Aviso KB, Le DQ, Kojima N, Tokai A. A linear programming input-output model for mapping low-carbon scenarios for Vietnam in 2030. Sustain Prod Consump. 2018;16:134–40.
4. Zhang WW, Zhao B, Gu Y, Sharp B, Xue SC, Liou KN. Environmental impact of national and subnational carbon policies in China based on a multi-regional dynamic CGE model. J Environ Manage. 2020;270: 110901.
5. Jiang MD, Huang YM, Bai Y, Wang Q. How can Chinese metropolises drive global carbon emissions? Based on a nested multi-regional input-output model for China. Sci Total Environ. 2023;856: 159094.
6. Danish Ozcan B, Ulucak R. An empirical investigation of nuclear energy consumption and carbon dioxide (CO2) emission in India: bridging IPAT and EKC hypotheses. Nucl Eng Technol. 2021;53(6):2056–65.
7. Zhang SS, Huo ZG, Zha CC. Building carbon emission scenario prediction using STIRPAT and GA-BP neural network model. Sustainability. 2022;14(15):9369.
8. Dong F, Yu B, Hadachin T. Drivers of carbon emission intensity change in China. Resour Conserv Recyl. 2018;129:187–201.
9. Xia Y, Wang HJ, Liu WD. The indirect carbon emission from household consumption in China between 1995–2009 and 2010–2030: A decomposition and prediction analysis. Comput Ind Eng. 2019;128:264–76.
10. Acheampong AO, Boateng EB. Modelling carbon emission intensity: application of artificial neural network. J Clean Prod. 2019;225:833–56.
11. Heydari A, Garcia DA, Keynia F, Bisegna F. Renewable energies generation and carbon dioxide emission forecasting in microgrids and national grids using GRNN-GWO methodology. Energy Procedia. 2019;159:154–9.

12. Wen L, Cao Y. Influencing factors analysis and forecasting of residential energy-related CO2 emissions utilizing optimized support vector machine. J Clean Prod. 2020;250: 119492.
13. Sun W, Huang CC. Predictions of carbon emission intensity based on factor analysis and an improved extreme learning machine from the perspective of carbon emission efficiency. J Clean Prod. 2022;338: 130414.
14. Yang M, Liu YS. Research on the potential for China to achieve carbon neutrality: a hybrid prediction model integrated with Elman neural network and sparrow search algorithm J. Environ Manage. 2023;329: 117081.
15. Kong F, Song JB, Yang ZZ. A novel short-term carbon emission prediction model based on secondary decomposition method and long short-term memory network. Environ Sci Pollut Res. 2022;29:64983–98.
16. Li XM, Zhao ZG, Zhao YF, Zhou SW, Zhang Y. Prediction of energy-related carbon emission intensity in China, America, India, Russia, and Japan using a novel self-adaptive grey generalized Verhulst model. J Clean Prod. 2023;423: 138656.
17. Gu HL, Wu LF. Pulse fractional grey model application in forecasting global carbon emission. Appl Energy. 2024;358: 122638.
18. Jiang JM, Zhang M, Huang ZY. A new adaptive grey prediction model and its application. Alex Eng J. 2025;120:515–22.
19. Zhou WJ, Chang JX, Zuo WZ, Wang FF. A seasonal grey model for forecasting energy imports demand from information differences perspective. Appl Math Model. 2025;140: 115907.
20. Zhou WJ, Chang JX, Jiang HM, Ding S, Jiang RR, Guo XP. A novel grey seasonal model with time power for energy prediction. Expert Syst Appl. 2025;259: 125356.
21. Wang Y, Yang ZS, Fan N, Wen SX, Kuang WY, Yang M, Li HL, Narayanan G, Sapnken FE. A novel fractional nonlinear discrete grey model with kernel-Markov adaptation for clean energy forecasting. Energy. 2025;323: 135888.
22. Zhou SW, Zhao YF, Li XM, Han R. A novel nonlinear time-varying grey prediction framework for green transformation of manufacturing industry: modeling of a non-equidistant perspective. Comput Ind Eng. 2025;203: 111068.
23. Yan SL, Peng MN, Wu LF, Xiong PP. A novel structural adaptive seasonal grey Bernoulli model in natural gas production forecasting. Eng Appl Artif Intell. 2025;148:110407. https://doi.org/10.1016/j.engappai.2025.110407.
24. Hao YW, Ma X, Song LL, Xiang YS. A residual learning-based grey system model and its applications in Electricity Transformer's Seasonal oil temperature forecasting. Eng Appl Artif Intell. 2025;147: 110260.
25. Li C, Liu SF, Yang YJ. Assessing numerical error bound of classic grey prediction model: an application to the transport performance of China's civil aviation industry. Expert Syst Appl. 2025;276: 127103.
26. Wang Y, Wang YH, Zhang ZJ, Sun L, Yang R, Sapnken FE, Xiao WL. A novel fractional-order kernel regularized non-homogeneous grey Riccati model and its application in oil reserves prediction. Energy. 2025;316: 134675.
27. Guo SD, Jia J, Han X, Geng SS. A nonlinear multivariate grey Bernoulli model for predicting innovation performance in high-tech industries. Commun Nonlinear Sci Numer Simul. 2025;143: 108636.
28. Liu XM, Li SH, Gao MN. A discrete time-varying grey Fourier model with fractional order terms for electricity consumption forecast. Energy. 2024;296: 131065.
29. Xu Y, Lin T, Du P, Wang JZ. An innovative interval grey model for construction waste forecasting. Appl Math Model. 2024;126:22–51.
30. Xiong PP, Zeng XS, W LP, Shu H. A fluctuation data grey model and its prediction of rainstorm days. Appl Math Model. 2024;127:767–783.
31. Wang SW, Xiao XP, Ding Q. A novel fractional system grey prediction model with dynamic delay effect for evaluating the state of health of lithium battery. Energy. 2024;290: 130057.
32. Wang YH, Liu Q, Tang JR, Cao WB, Li XZ. Optimization approach of background value and initial item for improving prediction precision of GM(1,1) model. J Syst Eng Electron. 2014;25:77–82.
33. Zhang W, Xiao R, Shi B, Zhu HH, Sun YJ. Forecasting slope deformation field using correlated grey model updated with time correction factor and background value optimization. Eng Geol. 2019;260: 105215.
34. Duan HM, Luo XL. Grey optimization Verhulst model and its application in forecasting coal-related CO2 emissions. Environ Sci Pollut Res. 2020;27:43884–905.
35. Wang HP, Zhang Z. Forecasting Chinese provincial carbon emissions using a novel grey prediction model considering spatial correlation. Expert Syst Appl. 2022;209: 118261.
36. Wu LF, Liu SF, Yao LG, Yan SL, Liu DL. Grey system model with the fractional order accumulation. Commun Nonlinear Sci Numer Simul. 2013;18(7):1775–85.
37. Zeng B, Liu SF. A self-adaptive intelligence gray prediction model with the optimal fractional order accumulating operator and its application. Math Methods Appl Sci. 2017;40(18):7843–57.
38. Wu WQ, Ma X, Zeng B, Wang Y, Cai W. Forecasting short-term renewable energy consumption of China using a novel fractional nonlinear grey Bernoulli model. Renew Energy. 2019;140:70–87.
39. Wang HP, Zhang Z. A novel grey model with conformable fractional opposite-direction accumulation and its application. Appl Math Model. 2022;108:585–611.
40. Mao S, Kang Y, Zhang Y, Xiao X, Zhu H. Fractional grey model based on non-singular exponential kernel and its application in the prediction of electronic waste precious metal content. ISA Trans. 2020;107:12–26.
41. Ma X, Wu WQ, Zeng B, Wang Y, Wu X. The conformable fractional grey system model. ISA Trans. 2020;96:255–71.
42. Xie WL, Wu WZ, Liu C, Gohd M. Generalized fractional grey system models: the memory effects perspective. ISA Trans. 2022;126:36–46.
43. Chen JK, Wu ZP. A positive real order weakening buffer operator and its applications in grey prediction model. Appl Soft Comput. 2021;99: 106922.
44. Xie WL, Wu WZ, Liu C, Zhao JJ. Forecasting annual electricity consumption in China by employing a conformable fractional grey model in opposite direction. Energy. 2020;202: 117682.
45. Wang Y, Chi P, Nie R, Ma X, Wu WQ, Guo BH. Self-adaptive discrete grey model based on a novel fractional order reverse accumulation sequence and its application in forecasting clean energy power generation in China. Energy. 2022;253: 124093.
46. Liu LY, Chen Y, Wu LF. The damping accumulated grey model and its application. Commun Nonlinear Sci Numer Simul. 2020;95: 105665.
47. Zhu HG, Liu C, Wu WZ, Xie WL, Lao TF. Weakened fractional-order accumulation operator for ill-conditioned discrete grey system models. Appl Math Model. 2022;111:349–62.
48. Wang Y, Wang L, Ye LL, Ma X, Wu WQ, Yang ZS, He XB, Zhang L, Zhang YY, Zhou Y, Luo YX. A novel self-adaptive fractional multivariable grey model and its application in forecasting energy production and conversion of China. Eng Appl Artif Intel. 2022;115: 105319.
49. Dang YG, Zhang YF, Wang JJ. A novel multivariate grey model for forecasting periodic oscillation time series. Expert Syst Appl. 2023;211: 118556.
50. He XB, Wang Y, Zhang YY, Ma X, Wu WQ, Zhang L. A novel structure adaptive new information priority discrete grey prediction model and its application in renewable energy generation forecasting. Appl Energy. 2022;325: 119854.
51. Zhou WJ, Ding S. A novel discrete grey seasonal model and its applications. Commun Nonlinear Sci Numer Simul. 2021;93: 105493.
52. Ding S, Tao Z, Li RJ, Qin XH. A novel seasonal adaptive grey model with the data-restacking technique for monthly renewable energy consumption forecasting. Expert Syst Appl. 2022;208: 118115.
53. Wang Y, He XB, Zhang L, Ma X, Wu WQ, Nie R, Chi P, Zhang YY. A novel fractional time-delayed grey Bernoulli forecasting model and its application for the energy production and consumption prediction. Eng Appl Artif Intell. 2022;110: 104683.
54. Gao MY, Yang HL, Xiao QZ, Goh M. A novel method for carbon emission forecasting based on Gompertz's law and fractional grey model: evidence from American industrial sector. Renew Energy. 2022;181:803–19.
55. Zhou WJ, Pan J, Tao HH, Ding S, Chen L, Zhao XK. A novel grey seasonal model based on cycle accumulation generation for forecasting energy consumption in China. Comput Ind Eng. 2022;163: 107725.
56. Wu LF, Zhao HY. Discrete grey model with the weighted accumulation. Soft Comput. 2019;23:12873–81.
57. Li KL, Xiong PP, Wu YR, Dong Y. Forecasting greenhouse gas emissions with the new information priority generalized accumulative grey model. Sci Total Environ. 2022;807: 150859.
58. Xiong PP, Li KL, Shu H, Wang JJ. Forecast of natural gas consumption in the Asia-Pacific region using a fractional-order incomplete gamma grey model. Energy. 2021;237: 121533.

59. Wu WZ, Pang HD, Zheng CL, Xie WL, Liu C. Predictive analysis of quarterly electricity consumption via a novel seasonal fractional nonhomogeneous discrete grey model: a case of Hubei in China. Energy. 2021;229: 120714.
60. Gou XY, Zeng B, Gong Y. Application of the novel four-parameter discrete optimized grey model to forecast the wastewater discharged in Chongqing China. Eng Appl Artif Intell. 2022;107: 104522.
61. Wang Q, Li SY, Li RR, Ma ML. Forecasting US shale gas monthly production using a hybrid ARIMA and metabolic nonlinear grey model. Energy. 2018;160:378–87.
62. Chen YH, Zhang C, He KJ, Zheng AB. Multi-step-ahead crude oil price forecasting using a hybrid grey wave model. Physica A. 2018;501:98–110.
63. Serge G, Gaston TJ, Wilfried ATE, Monkam L. Forecast of electricity consumption in the Cameroonian residential sector by Grey and vector autoregressive models. Energy. 2021;214: 118791.
64. Song ZG, Feng W, Liu WW. Interval prediction of short-term traffic speed with limited data input: application of fuzzy-grey combined prediction model. Expert Syst Appl. 2022;187: 115878.
65. Liu Y, Wu C, Wen J, Xiao X, Chen Z. A grey convolutional neural network model for traffic flow prediction under traffic accidents. Neurocomputing. 2022;500:761–75.
66. Wang ZX, He LY, Zhao YF. Forecasting the seasonal natural gas consumption in the US using a gray model with dummy variables. Appl Soft Comput. 2021;113: 108002.
67. Zhang Z, Wang HP. A grey breakpoint prediction model and its application in forecasting and policy evaluation. Eng Appl Artif Intell. 2023;126: 106784.
68. Deng J. Control problems of grey systems. Syst Control Lett. 1982;5:288–94.
69. Wu LF, Liu SF, Yao LG, Yan SL, Liu DL. Grey system model with the fractional-order accumulation. Commun Nonlinear Sci Numer Simul. 2013;18(7):1775–85.

Publisher's Note